

Advanced Carbon Capture for steel industries integrated in CCUS Clusters

Innovation Action

This project has received funding from the European Union's Horizon 2020 research and innovation programme under the Grant Agreement No 884418.

D3.6 - Techno-economic assessment of the C⁴U technologies within the steel plant (Task 3.4)

Work Package: 3

Due date of deliverable: month 57

Actual submission date: January 31st 2025

Start date of project: 1st April 2020 Duration: 60 months Lead beneficiary for this deliverable: Politecnico di Milano

Authors: Nicola Zecca (POLIMI) , Santiago Zapata Boada (UNIMAN)

Contributors: Giampaolo Manzolini (POLIMI), Vincenzo Spallina

Reviewers: Richard Porter

Table of Contents

Versio	on log	3
Execu	tive Summary	4
Prod	lucts valorisation according to the industrial cluster layout	5
Conte	ent	10
Abstrac	ot	11
1 In	troduction	11
1.1	The DISPLACE technology	15
1.2	The CASOH technology	15
1.3	Aim of the work	16
2 M	lethod	16
2.1	Analysed plants	17
2.	1.1 Base BF-BOF plant	17
2.	1.2 Reference BF-BOF plant	18
2.	1.3 C ⁴ U steel plant	18
2.2	DISPLACE modelling and process integration	19
2.3	CASOH modelling and process integration	21
2.4	Other components modelling	23
2.5	General assumptions	24
2.6	Methodology for the economic assessment	24
2.7	Key Performance Indicators	25
3 R	esults	27
3.1	DISPLACE performances	27
3.2	CASOH performances	27
3.3	Overall plant performance and emissions for different level of integration	28
4 C	onclusions	34
Acknow	wledgements	35
Append	lix A	36
	lix B	
Bibliog	raphy	41

Version log

Version	Date	Released by	Nature of Change
0.1	28/01/2025	N. Zecca (Polimi)	First version
1.1	18/02/2025	N. Zecca (Polimi)	Reviewed implementing comments received by Richard Porter and Marcos Cano Bertiz

Executive Summary

This deliverable presents the final techno-economic assessment of the C⁴U technologies when implemented in steel plants.

The core of the deliverable is the paper that is submitted to the International Journal of Greenhouse Gas Control for its publication in parallel to its upload on the participant portal, The paper focuses on the optimal system integration with the minimum fossil fuel import and maximum CO₂ avoidance, however additional hydrogen use cases are also presented in the second part of this executive summary.

The deliverable was delayed with respect to the original plan (by around 1 Month) because the first configuration of the CASOH technology was too expensive and not competitive form a cost perspective (see deliverable 3.5). Therefore, it was necessary to implement a new design to reduce the costs with limited impacts on the process performance. Some iterations between the different partners involved in CASOH design (CSIC, UNIMAN), CASOH costing (WOOD) and overall system integration (POLIMI) were necessary to identify the optimal configuration requiring additional time and efforts than initially planned.

The final lay-out considers the DISPLACE process applied to the sinter plant, reheating ovens and coke oven flue gases, while the CASOH works with the blast furnace and basic oxygen furnace gases.

The analysis is performed considering actual CO₂ footprint of the electricity purchased (250 kg_{CO2}/MWh) and a more optimistic future scenario with fully renewable electricity leading to significant variation in the Key Performance Indicators (KPIs).

Overall, the CASOH process contributes to avoid around 30% of CO $_2$ emissions, while DISPLACE around 42% when applied to all the above considered gases. These numbers correspond to the case where all the additional electricity purchased from the grid is renewable and reduces by 20% if the electricity has a carbon footprint. Overall, the C 4 U cases have a CO $_2$ avoidance which is significantly higher than the reference commercial technology. The SPECCA of C 4 U is strongly related to the assumption about the electricity purchased from the grid as it can range from -4.2 GJ/t_{CO2} for the CASOH only with green electricity up to 3.1 GJ/t_{CO2} when all the streams are processed for CO $_2$ capture and the electricity is not green.

Finally, the resulting cost of CO_2 avoided of the C^4U is strongly dependent on the cost of electricity and NG assumed. In the case of NG and electricity prices equal to $50 \, \text{€/MWh}$ and $125 \, \text{€/MWh}_{\text{el}}$, the C^4U technology is more expensive than the reference case mainly because the CO_2 avoided is more than twice with consequent penalties (result equal to 138 $\, \text{€/t}_{CO2,avoided}$). In the case of NG and electricity prices equal to $50 \, \text{€/MWh}$ and $50 \, \text{€/MWh}_{\text{el}}$ (representing a situation with a higher renewable energy penetration as in Scandinavian areas), the C^4U is cheaper than the reference case with values which can be as low as $28 \, \text{€/t}_{CO2}$.

Products valorisation according to the industrial cluster layout

Additional analyses with respect to the ones presented in the paper considers opportunities of using the available gas streams in the steel plant for pure H_2 production, gas-to-liquids synthesis in addition to the CO₂ pipeline and storage. In the C⁴U case the H₂rich from CASOH is used internally in the steel plant as low-carbon fuel. In the following analysis additional cases were addressed: i) no internal use of H₂-rich mixture from CASOH in the steel plant with consequent maximum export, ii) production and export of pure hydrogen, iii) synthesis and export of methanol. The analysed alternatives are shown in Figure EX.1. In the first case, the H₂-rich mixture produced from CASOH, differently from the cases presented in section 3.3 where it produces the steam necessary by DISPLACE technology, is exported and used as an alternative fuel to natural gas. The second case is like the first one, but the H₂-rich mixture produced from CASOH is purified before its export. The H_2 -rich mix is firstly compressed from 8.2 bar to 50 bar and then sent to the purification step performed through polymeric membrane. The permeated pure H2 is then compressed to 65 bar for the final export. In the third case, the pure H_2 of the second case and CO_2 are compressed at 90 bar and then synthesized as methanol. The power demand of the compressors was computed in Aspen Plus V14 using MCompr block, with 3-stages, a cooling temperature of 35 °C, polytropic and mechanical efficiencies of the stages equal to 0.85 and 0.95 respectively and selecting the RKS-BM method. As previously mentioned, a polymeric membrane was incorporated into the plant layout. A 1-D model of the membrane was developed to calculate the necessary membrane area to achieve the desired separation target. The permeability of hydrogen was computed using equation (ES.1) (Budhi et al., 2020), which is commonly referred as Richardson's equation (De Falco et al., 2011).

$$J_{H_2} \left[\frac{\text{mol}}{S} \right] = P_{H_2}^0 / \delta \, e^{\left(-\frac{E_a}{RT} \right)} \left[P_{H_2, \text{retentate}}^n - P_{H_2, \text{permeate}}^n \right] \tag{ES.1}$$

Where $P_{H_2}^0/\delta$ is the hydrogen permeance, E_α is the activation energy $[J \cdot mol^{-1}]$, R is the ideal gas constant $[J \cdot mol^{-1} \cdot K^{-1}]$, T is the absolute temperature of system [K], and δ is the membrane thickness [m]. Based on the findings of (Lu et al., 2021) the value of $P_{H_2}^0/\delta$ ranges between 10^{-9} and $3 \cdot 10^{-7}$ mol· $m^{-2} \cdot s^{-1} \cdot Pa^{-1}$. For this study, an intermediate value of 10^{-8} mol·m⁻²·s⁻¹·Pa⁻¹ was chosen. The activation energy E_α was set to 0 $J \cdot mol^{-1}$ while the exponent "n" is equal to 1.

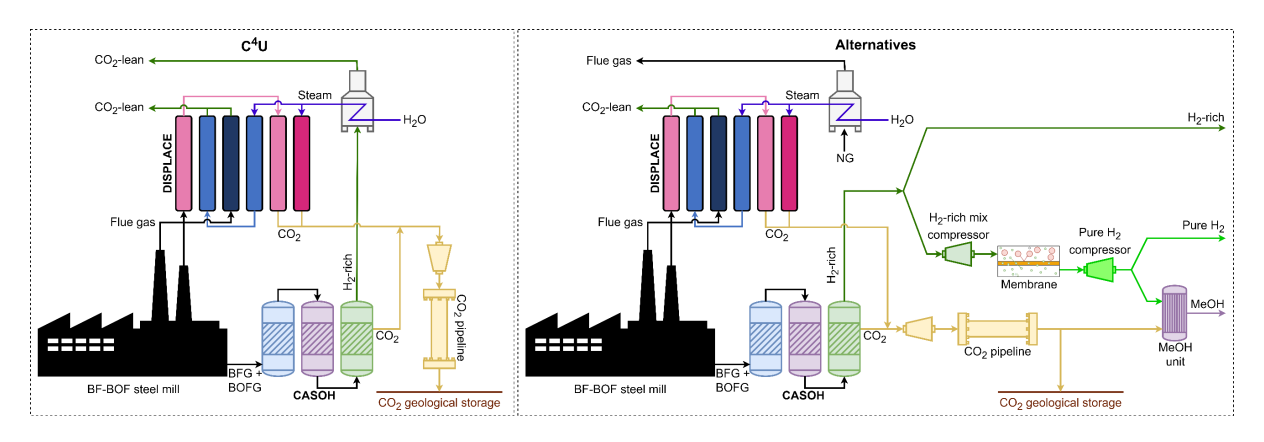


Figure EX.1: C⁴U steel plant (left) and alternatives for H₂-rich stream usage (right).

In the techno-economic analysis, the NG and emissions avoided, compared to reference cases of hydrogen and methanol production from natural gas, are accounted for. The same methodology described in previous sections was applied, with additional assumptions outlined in Table EX.1 together with the CAPEX following the methodology described in section 2.6 and using equation (B.1). Methanol is assumed to be sold at the same price of blue methanol. (IEAGHG Technical Report, 2017), with costs converted from USD to Euros and adjusted for inflation. In the report the dependence of blue methanol cost on NG and electricity price is given. In both cases a linear relation is show. The sensitivity of the levelized cost of methanol (LCOMeOH) to electricity prices is analysed for a fixed natural gas price of 6 €/GJ, with electricity prices ranging from 20 €/MWh to 100 €/MWh. The equation of this linear relationship is derived and used to compute the intercept for the sensitivity of LCOMeOH to natural gas prices at varying electricity prices. The LCOMeOH dependence on NG price is given for a constant electricity price of 80 €/MWh. The slope of the linear trend remains unchanged for different electricity prices. However, the relationship is adjusted upward or downward depending on the electricity price considered.

Table EX.1: Assumptions used for the techno-economic analysis of pure H₂ and methanol production.

Parameter	Unit	Value	Reference
Hydrogen permeance in membrane	mol·m ⁻² ·s ⁻¹ ·Pa ⁻¹	10-8	(Lu et al., 2021)
CO + CO ₂ conversion to MeOH	mol/mol	0.97	
CO ₂ footprint of grey H ₂	$t_{\text{CO2}}/t_{\text{H2}}$	2.55	(Lewis et al., 2022)
NG consumption of grey H2 (feedstock + fuel)	t_{NG}/t_{H2}	3.53	(Lewis et al., 2022)
Electricity consumption of grey H ₂	$GJ_{\text{el}}/t_{\text{H2}}$	2.33	(Lewis et al., 2022)
MeOH distillation process steam demand	$t_{\text{steam}}/t_{\text{MeOH}}$	0.432	(Gentile et al., 2022)
MeOH distillation process steam demand	$GJ/t_{\mbox{\tiny MeOH}}$	1.16	(Gentile et al., 2022)
CO ₂ footprint of grey MeOH	$t_{\text{CO2}}/t_{\text{MeOH}}$	0.62	(Hamelinck and Bunse, 2022)
NG consumption of grey MeOH (feedstock + fuel)	$t_{\text{NG}}/t_{\text{MeOH}}$	0.65	(IEAGHG Technical Report, 2017)
Electricity consumption of grey MeOH	GJ_{el}/t_{MeOH}	0.319	(IEAGHG Technical Report, 2017)
CAPEX of the membrane	€/m²	50	(Sandhya Rani and Kumar, 2021)
Membrane lifetime	years	6	
CAPEX of a 300 t/d MeOH synthesis unit	M€	44.1	(Gentile et al., 2022)
CAPEX of a 10 MW H ₂ compressor	M€	13.48	(Lewis et al., 2022)

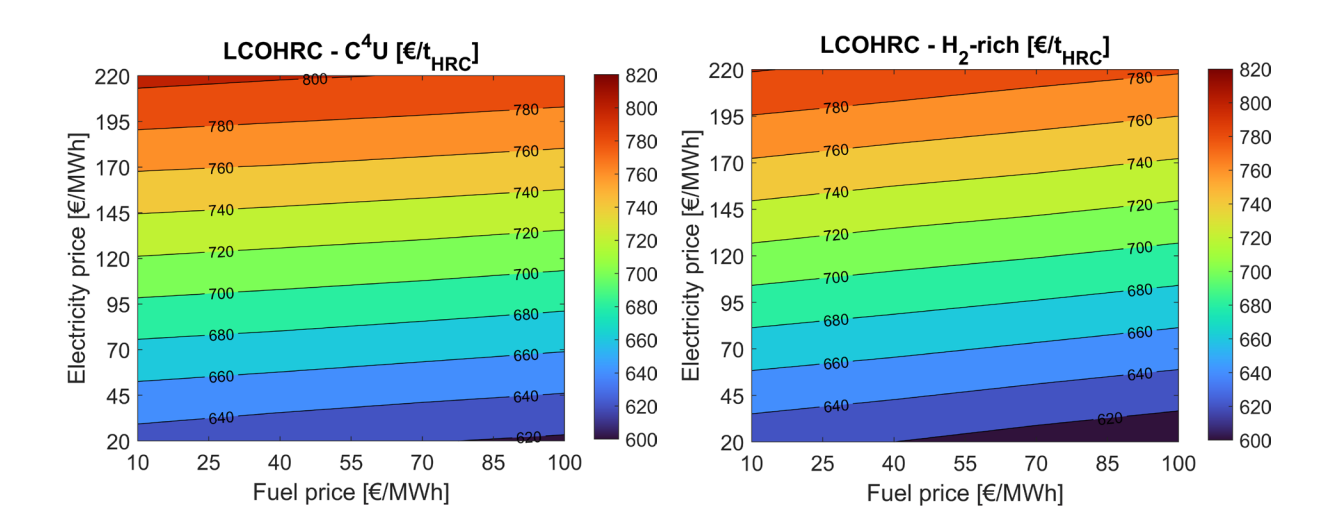
Parameter	Unit	Value	Reference	
O&M H ₂ /MeOH synthesis equipment	%·CAPEX	5		
Additional personnel	-	15		
Pure H ₂ selling price	€/kg _{H2}	1.25·LCOH		

The results of techno-economic analysis considering the maximum export of H_2 -rich mix from CASOH (" H_2 -rich"), methanol ("MeOH") and pure H_2 ("Pure H_2 ") production are given in Table EX.2. The H_2 -rich mix is considered as a replacement of natural gas without CO_2 emissions, while H_2 pure is supposed to be used for other purposes such as for synthesis of chemicals. In Table EX.2, negative values are associated to the export of streams, and they represent a reduction of CO_2 emissions, savings of primary energy consumption or revenues generating for the selling of by-products. In general, all the cases present similar results as selling more H_2 leads to more NG import to the plant which is balanced by the avoided emissions for hydrogen utilization. Similarly, there is no relevant difference in the cost of HRC provided that the results are strongly dependent on the economic assumptions made. Certainly, the cost of the products is strongly affected by the NG and electricity prices as reported in Figure EX.2.

Table EX.2: Results of the techno-economic analysis assuming electricity and natural gas prices equal to 125 €/MWh_{el} and 50 €/MWh_{LHV} respectively and considering a carbon footprint of purchased electricity equal to 250 kg_{CO2}/MWh_{el}.

Parameter	Unit	C⁴U	H ₂ -rich	Pure H ₂	MeOH
H ₂ -rich mix export	kg/t _{HRC}	60.9	200.1		
H ₂ -rich mix to membrane	$kg/t_{\mbox{\tiny HRC}}$			200.1	200.1
H ₂ in H ₂ -rich mix	$kg/t_{\mbox{\tiny HRC}}$	7.6	7.6	7.6	7.6
H ₂ pure membrane outlet	$kg/t_{\mbox{\tiny HRC}}$			6.5	6.5
H ₂ pure export	$kg/t_{\mbox{\tiny HRC}}$			6.5	
MeOH export	$kg/t_{\mbox{\tiny HRC}}$				33.4
Additional NG import for steel plant	$kg/t_{\mbox{\tiny HRC}}$		14.5	14.5	14.5
NG import for steam generation in MeOH unit	$kg/t_{\mbox{\tiny HRC}}$				0.9
Compression of H ₂ -rich mix upstream the membrane	MW			7.2	7.2
Compression of pure H ₂ downstream membrane	MW			5.9	6.5
Steam to MeOH unit for distillation	MW				4.2
CAPEX membrane	M€			21.5	21.5
CAPEX compressor H ₂ -rich mix	M€			9.7	9.7
CAPEX compressor pure H ₂	M€			8.5	9.1
CAPEX MeOH unit	M€				45.0
CO ₂ to pipeline	kg _{co2} /t _{HRC}	1502.2	1502.2	1502.2	1454.9
CO ₂ emissions reduction for avoiding NG combustion	kg _{co2} /t _{HRC}	-17.2	-56.6		
CO ₂ emissions reduction for avoiding grey H ₂ production	$kg_{\text{CO2}}/t_{\text{HRC}}$			-16.6	
CO ₂ emissions reduction for avoiding grey MeOH production	kg _{co2} /t _{HRC}				-20.7
CO ₂ emissions NG combustion in steel plant	$kg_{\text{CO2}}/t_{\text{HRC}}$		39.4	39.4	39.4
$\ensuremath{\text{CO}_2}$ emissions NG combustion for steam generation in MeOH unit	kg _{co2} /t _{HRC}				2.4
CO ₂ emissions electricity compressor of H ₂ -rich mix	$kg_{\text{CO2}}/t_{\text{HRC}}$			4.7	4.7
CO ₂ emissions electricity compressor of pure H ₂	kg _{co2} /t _{HRC}			3.8	4.2

Parameter	Unit	C⁴U	H₂-rich	Pure H ₂	МеОН
Total CO ₂ emissions	kg _{co2} /t _{HRC}	833	833	882	881
CO ₂ emissions difference with respect to C ⁴ U case	kg _{co2} /t _{HRC}		0.0	48.5	47.2
CO ₂ avoidance with respect to base steel BF-BOF plant	%	60.4	60.4	58.1	58.2
PEC saved for avoiding NG combustion	$GJ/t_{\mbox{\tiny HRC}}$	-0.3	-1.0		
PEC saved for avoiding grey H ₂ production	$GJ/t_{\mbox{\tiny HRC}}$			-1.1	
PEC saved for avoiding grey MeOH production	$GJ/t_{\mbox{\tiny HRC}}$				-1.0
PEC of additional NG consumption	$GJ/t_{\mbox{\tiny HRC}}$		0.7	0.7	0.7
PEC of additional electricity	$GJ/t_{\mbox{\tiny HRC}}$			0.1	0.2
Total PEC	$GJ/t_{\mbox{\tiny HRC}}$	25.2	25.2	25.2	25.4
SPECCA	GJ/t _{co2}	3.1	3.1	3.2	3.3
Expenses for additional NG consumption	€/t _{HRC}		9.4	9.4	10.0
Expenses for additional electricity	€/t _{HRC}			4.3	4.5
CAPEX membrane	€/t _{HRC}			0.6	0.6
CAPEX compressor of H ₂ -rich mix	€/t _{HRC}			0.3	0.3
CAPEX compressor of pure H ₂	€/t _{HRC}			0.3	0.3
CAPEX MeOH unit	€/t _{HRC}				1.3
O&M additional units	€/t _{HRC}			0.1	0.1
Additional personnel	€/t _{HRC}			0.3	0.3
Revenues for selling H ₂ -rich mix	€/t _{HRC}	-7.9	-26.0		
Revenues for selling pure H ₂	€/t _{HRC}			-28.0	
Revenues from selling MeOH	€/t _{HRC}				-23.3
LCOHRC	€/t _{HRC}	718.3	709.6	713.4	720.3
LCOHRC difference with respect to C ⁴ U	€/t _{HRC}		-8.6	-4.8	2.1
Cost of CO ₂ avoided	€/tco2	164.7	157.9	167.3	172.7
Cost of CO ₂ avoided difference with respect to C ⁴ U	€/tco2		-6.8	2.6	8.0



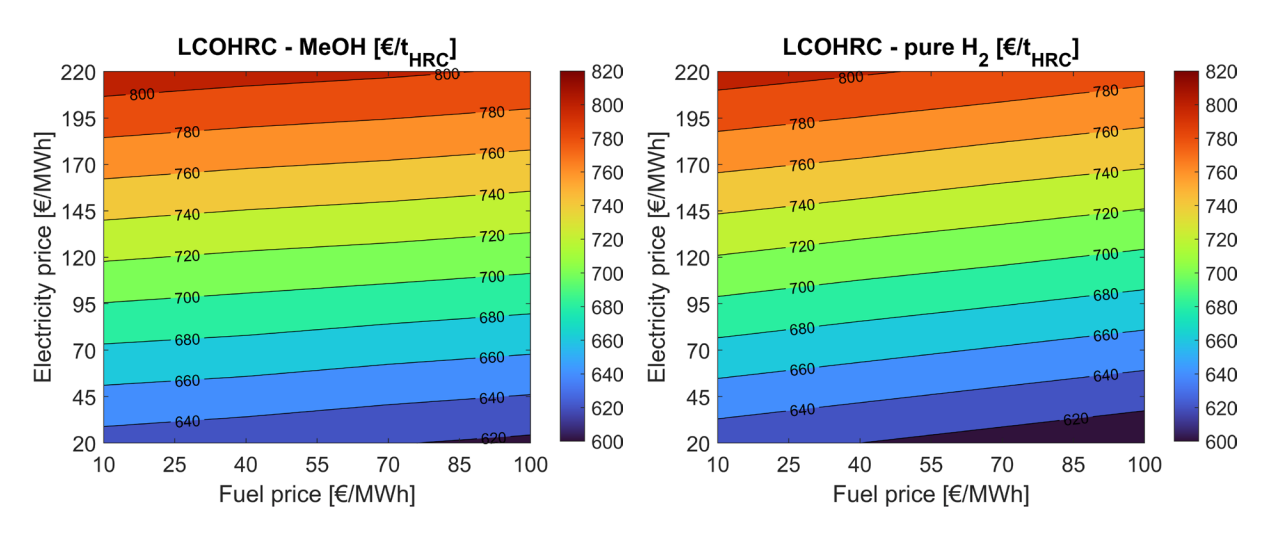


Figure EX.2: LCOHRC. Sensitivity analysis on natural gas and electricity prices.

Content

The following section includes the paper submitted to the International Journal of Greenhouse Gas Control for publication.

Integration of CASOH and DISPLACE technologies in a steel plant for the mitigation of CO₂ emissions

Nicola Zecca^{1a}, Santiago Zapata Boada², Vincenzo Spallina², Giampaolo Manzolini¹

¹Politecnico di Milano, Dipartimento di Energia, via Lambruschini 4, 20126, Milano, Italy ²Department of Chemical Engineering, University of Manchester, Manchester M13 9PL, UK

a) Corresponding author: nicola.zecca@polimi.it

Abstract

Given the severe climate crisis and the urgent need to limit the adverse effects of global warming, drastic changes are required across various industries Among them, the iron and steel sector is a major contributor to greenhouse gas emissions, accounting for approximately 7% of global emissions. This study proposes integrating innovative carbon capture technologies, such as DISPLACE and CASOH, into the conventional BF-BOF (Blast Furnace-Basic Oxygen Furnace) steelmaking process. A comprehensive techno-economic analysis was conducted, supported by simulations performed in Aspen Plus, to optimize the integration of these technologies. The study suggests a redesigned gas distribution system within the BF-BOF steel plant, incorporating oxy-fired units to facilitate post-combustion carbon capture and minimize the plant emissions. The analysis reveals that employing CASOH for pre-combustion CO₂ capture to decarbonize a mixture of BFG (Blast Furnace Gas) and BOFG (Basic Oxygen Furnace Gas), combined with DISPLACE for decarbonizing flue gases from hot stoves, sinter plant, and reheating ovens, 72% reduction in CO₂ emissions and a SPECCA around 0 GJ/t_{CO₂} can be achieved. This is attainable within a renewable electricity scenario, at a cost of €138 per ton of CO₂ avoided. Lower CO₂ avoidance can also be achieved by treating less exhaust gases with reduction in both SPECCA and costs.

Key words: CASOH; DISPLACE; steel; CCS; techno-economic analysis

1 Introduction

The iron and steel industry which account for about 7% of global direct energy-related CO₂ emissions faces significant challenges in reducing emissions due to its heavy reliance on fossil fuels, particularly coal, in the blast furnace-basic oxygen furnace (BF-BOF) steelmaking route, which currently dominates the steel market, accounting for 70% of global steel production and 90% of primary production (International Energy Agency, 2020). Another primary production method is the direct reduced iron-electric arc furnace (DRI-EAF) route, which differs from BF-BOF by using high-quality DRI pellets instead of raw iron ore. Reduction occurs in a solid state in the DRI furnace before melting in the EAF, often combined with scrap. This route utilizes hydrogen and carbon monoxide as reducing agents, with natural gas predominantly used to generate the required syngas (International Energy Agency, 2020). Secondary steel production which represents approximately 22% of total steel production, primarily relies on electricity to melt scrap in electric arc furnaces which operate at high temperatures facilitated by conductive graphite electrodes (International Energy Agency, 2020).

Integrating carbon capture technologies into steel production processes is essential for progressing towards a net-zero emissions future. (Perpiñán et al., 2023) conducted a systematic review of peer-reviewed articles focused on the integration of carbon capture technologies in the BF-BOF steelmaking route, categorizing the carbon capture technologies into four main groups: i) post-combustion (chemical absorption, membranes), ii) looping processes (calcium looping, chemical looping, other looping processes), iii) oxygen blast furnaces and top-gas recycling, and iv) pre-combustion (chemical absorption, adsorption, membranes, SEWGS). These technologies are compared considering 6 KPIs: thermal penalty (GJ/t_{CO2}), electrical penalty (GJ/t_{CO2}), economic cost (\$/t_{CO2}), CO₂ emission reduction, (kg/t_{HM}), CO₂ purity (%) and TRL as reported in Table 1.

Nomenclatu	re		
Acronyms		RO	Reheating Ovens
ASU	Air Separation Unit	SEWGS	Sorption Enhanced Water Gas Shift
BF	Blast Furnace	SPECCA	Specific PEC per unit of CO2 Avoided [GJ/tCO2
BFG	Blast Furnace Gas	TAC	Total Annualised Cost [M€/y]
BOF	Basic Oxygen Furnace	TEC	Total Equipment Cost [€]
BOFG	Basic Oxygen Furnace Gas	TGR	Top Gas Recycling
CCA	Cost of CO ₂ Avoided [€/t _{CO2}]	TPC	Total Plant Cost [€]
CCR	Carbon Capture Ratio [%]	TRL	Technology Readiness Level
COG	Coke Oven Gas	WGS	Water Gas Shift
CP	Carbon Purity [%]		
DRI	Direct Reduced Iron	Symbols	
EAF	Electric Arc Furnace	e_{CO2}	Specific CO ₂ emissions [t _{CO2} /t _{product}]
FCF	Fixed Charge Factor	h_{eq}	Equivalent hours [h/y]
HM	Hot Metal	ṁ	Mass flowrate [kg/s]
HS	Hot Stoves	p	Pressure [bar]
KPI	Key Performance Indicators	Δp	Pressure drops [bar]
LCOH	Levelized Cost of Hydrogen [€/kg _{H2}]	T	Temperature [°C]
LCOHRC	Levelized Cost of Hot Rolled Coil [€/t _{HRC}]	ΔT	Temperature difference [°C]
MDEA	Methyldiethanolamine		
MEA	Monoethanolamine	Subscripts	
MP	Medium Pressure	h	Hydraulic
MPS	Medium Pressure Steam	is	Isentropic
MPW	Medium Pressure Water	m	Mechanical
NG	Natural Gas	p	Polytropic
NGCC	Natural Gas Combined Cycle	th	Thermal
OBF	Oxy Blast Furnace		
PEC	Primary Energy Consumption [GJ/t _{HRC}]	Greek	
RES	Renewable Energy Sources	η	Efficiency [-]

Chemical absorption has been extensively investigated for post-combustion carbon capture from flue gases of hot-stoves (Chamchan et al., 2017; Cheng et al., 2010; Goto et al., 2011), of power plant (Gazzani et al., 2015; Manzolini et al., 2020; Sundqvist et al., 2018), and coke ovens (Oko et al., 2018; Wiley et al., 2011). To enhance CO₂ emission reductions, concurrent carbon capture from multiple sources has been studied (Arasto et al., 2013b; Yun et al., 2021). The most commonly examined amines are monoethanolamine (MEA) and methyldiethanolamine (MDEA) with other solvents seldomly addressed in literature.

Relatively few theoretical studies regarding the use of membranes are present in literature, due to the still low TRL of membranes in the iron and steel industry (Baker et al., 2018; Luca and Petrescu, 2021; Yun et al., 2021). However, membranes can achieve high CO₂ purity levels.

In the case of calcium looping, many studies consider the decarbonisation of various CO₂ sources, such as blast furnace gas (BFG), basic oxygen furnace gas (BOFG), coke oven gas (COG), or flue gas from hot stoves or lime kilns (Chisalita et al., 2019; Cormos et al., 2020a; Halmann and Steinfeld, 2015; Tian et al., 2018). Some studies have focused on applying the chemical looping concept for the combustion of coke oven gases (COG) without CO₂ emissions or for producing hydrogen for the steelmaking process (Katayama et al., 2020; Luo et al., 2018; Xiang and Zhao, 2018). Similarly, other looping processes have been evaluated for the decarbonization of BFG, BOFG, and COG (Fernández et al., 2020, 2017; Martínez et al., 2019, 2018a; Sun et al., 2020). However, in both cases, the TRL is still low.

Oxygen blast furnaces and top-gas recycling strategies are among the most widely investigated methods in the iron and steel industry for mitigating CO₂ emissions. These concepts were optimised and tested in the context of the ULCOS project (Arasto et al., 2014; Ho et al., 2013; Jin et al., 2016; Li et al., 2020; Qie et al., 2020; She et al., 2017; Tsupari et al., 2015; Zuo Guangqing and Hirsch A., 2009). In OBF, oxygen-enriched hot-blast air is used in the shaft furnace for coke combustion, resulting in a more CO₂-concentrated blast furnace top gas due to the reduced nitrogen content. The TGR concept involves recycling a portion of the top gas back to the blast furnace, after a CO₂ capture stage.

Chemical absorption technology is also studied in the steel industry for pre-combustion carbon capture configuration (Birat, 2010; Gazzani et al., 2015; Martinez Castilla et al., 2019; Sundqvist et al., 2018). MEA, MDEA and piperazine are the most investigated solvents.

In the case of adsorption, the vacuum-pressure swing adsorption process is the most investigated and is usually coupled with the TGR concept, processing blast furnace gas (Abdul Quader et al., 2016; Danloy G. et al., 2009; Jin et al., 2017; Kim et al., 2015; Quader et al., 2016; Sahu et al., 2015; She et al., 2017).

Membranes can also be used in pre-combustion mode (Chung et al., 2018a; Jeon et al., 2022; Li et al., 2022; Ramírez-Santos et al., 2018). According to (Hasan et al., 2012), membrane separation is preferable to amine scrubbing for CO₂ concentrations above 36%. Most studies focus on the decarbonization of BFG, demonstrating low costs but also indicating a low TRL.

Finally, the use of Sorption-Enhanced Water-Gas Shift (SEWGS) has been investigated for the pre-combustion decarbonization of gases typically used as fuel in the power plants of BF-BOF steel mills (Gazzani et al., 2015; Manzolini et al., 2020; Petrescu et al., 2019; van Dijk et al., 2018).

In general, the thermal penalty for various carbon capture technologies varies between 1.3 and 6.2 GJ/ $t_{\rm CO2}$ (Perpiñán et al., 2023). When it comes to electricity consumption, post-combustion chemical absorption, calcium looping, and pre-combustion chemical absorption generally have lower electricity requirements, averaging less than 1 GJ/ $t_{\rm CO2}$ because heat consumption is predominant, with most of electricity usage related to CO_2 compression (Perpiñán et al., 2023). On the other hand, technologies like membranes (post- and pre-combustion), and adsorption pre-combustion requires a compression step upstream the CO_2 capture process, leading to higher electricity penalties between 1 and 3 GJ/ $t_{\rm CO2}$ (Perpiñán et al., 2023). It must be noted that low energy penalty and low costs are typically associated to low TRL concepts, while higher penalties and costs are related to high TRL technologies.

Table 1: Main KPIs for carbon capture technologies integrated in steel plants.

CC technology	CO ₂ source	Thermal penalty [GJ/t _{CO2}]	Electrical penalty [GJ/t _{CO2}]	Cost [\$/t _{CO2}]	Emissions reduction [t _{CO2} /t _{steel}]	CO ₂ purity [%]	TRL	References
Post combustion								
- Chemical absorption	Hot-stoves, power plant, coke ovens, lime kilns, sinter plant	2.3 – 6.5	0.28 – 1.5	38 – 204	0.2 – 1.7	> 95	2-5	(Arasto et al., 2013a, 2013b; Biermann et al., 2019; Chamchan et al., 2017; Cheng et al., 2010; Chisalita et al., 2019; Cormos et al., 2020a; Cormos, 2016; Gazzani et al., 2015; Goto et al., 2011; Ho et al., 2011; Manzolini et al., 2020; Martínez et al., 2018b; Oko et al., 2018; Sundqvist et al., 2018; Tsupari et al., 2013; Wiley et al., 2011; Yun et al., 2021)
- Membrane	Hot-stoves, power plant, coke ovens, lime kilns, sinter plant	n/a	0.9 – 4.4	36 – 252.7	n/a	> 90	3 – 6	(Baker et al., 2018; Luca and Petrescu, 2021; Yun et al., 2021)
Looping processes								
- Calcium looping	BFG, BOFG, COG,	2.7 – 5.6	0.1 - 2.5	60.2 – 73.8	1 – 1.7	> 95	2 – 3	(Chisalita et al., 2019; Cormos et al., 2020a; Cormos, 2016; Halmann and Steinfeld, 2015; Tian et al., 2018; Xie et al., 2017)
	hot-stoves, lime kilns							
- Chemical looping	COG, sinter plant	n/a	n/a	n/a	n/a	90	2 – 4	(Katayama et al., 2020; Luo et al., 2018; Xiang and Zhao, 2018)
- Other processes	BFG, BOFG, COG	1.4 – 4.3	n/a	n/a	0.5 – 1.6	57 – 99.9	3 – 5	(Fernández et al., 2020, 2017; Martínez et al., 2019, 2018a; Sun et al., 2020)
TGR-OBF	BFG	0.3	1.4 - 5.6	50 – 90	0.1 - 0.6	n/a	2 – 6	(Arasto et al., 2014; Ho et al., 2013; Jin et al., 2016; Li et al., 2020; Qie et al., 2020; She et al., 2017; Tsupari et al., 2015; Zuo Guangqing and Hirsch A., 2009)
Pre-combustion								
- Chemical absorption	BFG, BOFG, COG	1.3 – 4.4	0.2 –1.2	40.6 – 97	0.6 – 1	> 90	2 – 6	(Birat, 2010; Chung et al., 2018b; Gazzani et al., 2015; Ho et al., 2011; Martinez Castilla et al., 2019; Onarheim and Arasto, 2016; Sundqvist et al., 2018)
- Adsorption	BFG, OBFG	n/a	0.4 - 2.7	60	0.5 - 1.2	> 79.9	2 – 6	(Abdul Quader et al., 2016; Danloy G. et al., 2009; Ho et al., 2013; Jin et al., 2017; Kim et al., 2015; Quader et al., 2016; Sahu et al., 2015; She et al., 2017)
- Membranes	BFG, BOFG	n/a	0.4 - 1.6	28.8 - 50.6	0.8	> 55	2 – 4	(Chung et al., 2018a; Jeon et al., 2022; Li et al., 2022; Ramírez-Santos et al., 2018)
- SEWGS	BFG, BOFG, COG	n/a	1.9 – 2.9	36.4	0.6 - 0.8	> 96.8	2 – 6	(Gazzani et al., 2015; Manzolini et al., 2020; Petrescu et al., 2019; van Dijk et al., 2018)

1.1 The DISPLACE technology

The DISPLACE technology (Downstream Integrated Steel Production with Advanced CO₂ Capture) is a multicolumn post-combustion CO₂ capture system. It operates on an isobaric concentration swing principle, delivering two separate product streams at unit operating pressure (Figure 1). In the feed step, CO₂ is adsorbed onto a sorbent, generating a CO₂-lean stream, while the sorbent is regenerated by displacing CO₂ with steam, resulting in a CO₂-rich product, without requiring pressure or temperature swings. In the process, the CO₂ is adsorbed onto the sorbent due to its high partial pressure. The sorbent commonly used is K-promoted hydrotalcite. To achieve a continuous process, the DISPLACE cycle development is based on the following constraints: i) one column always receives feed; ii) one column always produces the CO₂-lean product; iii) one column always produces the CO₂-rich product; iv) steam consumption is reduced by recycling Ads-1 within the cycle; v) CO₂ purity is increased by recycling Des-1 within the cycle. Compared to SEWGS, although the DISPLACE process operates at a lower pressure, it generates a CO₂-rich product at higher pressure. Details of the process can be found in (Zecca et al., 2025).

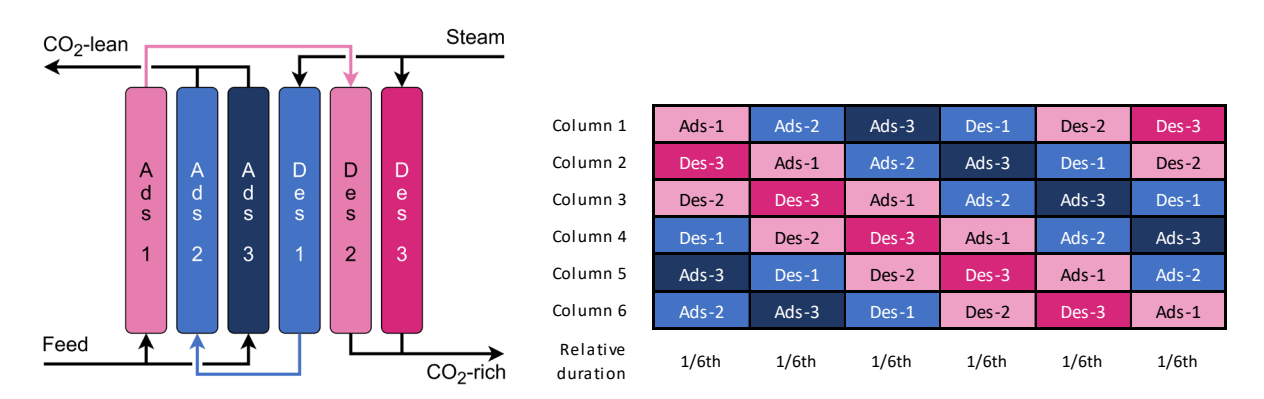


Figure 1: Six column DISPLACE process (left) and timing for a 6-column unit (right). The column names indicate which product gas they are producing. Reprinted from (Zecca et al., 2025).

1.2 The CASOH technology

Calcium looping has been extensively studied as post-combustion CO₂ capture technology in conventional power plants and biomass-driven systems. Additionally, its efficacy has been explored in hydrogen production within reforming processes, demonstrating significant benefits such as high CH₄ conversion efficiency and the production of high-purity hydrogen at temperatures below 650 °C (Masoudi Soltani et al., 2021; Yan et al., 2020). However, a critical challenge lies in the economic viability of regenerating CaCO₃, a crucial step in the calcium looping process. This regeneration process requires high temperatures exceeding 850 °C and necessitates either pure oxygen from an air separation unit (ASU) (Arias et al., 2013; Ströhle et al., 2014) or the integration of thermal storage mechanisms to transfer heat effectively from the carbonator to the calciner (Astolfi et al., 2021). Consequently, addressing the cost and energy demands of CaCO₃ regeneration is essential for the widespread adoption of calcium looping technology.

An alternative approach integrates calcium and chemical looping techniques using a copper-based oxygen carrier. Known as the calcium-copper (Ca-Cu) looping process, this method has been proposed by (Abanades et al., 2010) as a potential solution for addressing the energy demands associated to calcination. An innovative system configuration called Calcium Assisted Steel-mill Off-gas Hydrogen production (CASOH) incorporates Ca-Cu looping with the Sorption Enhanced Water Gas Shift (SEWGS) reaction. (Fernández et al., 2020) and (Grasa et al., 2023) have explored this configuration, highlighting its potential to achieve energy efficiency.

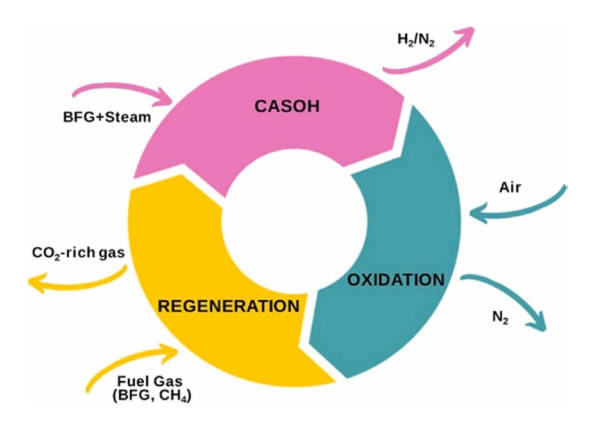


Figure 2: CASOH process concept for the production of H2 from BFG with CO2 capture. Reprinted from (Grasa et al., 2023).

1.3 Aim of the work

The objective of this study is to evaluate the optimal integration of DISPLACE and CASOH technologies into the layout of a conventional BF-BOF steel plant, with the aim of minimizing the carbon footprint of steel production. The DISPLACE technology is applied to the flue gases generated by hot stoves, reheating furnaces, and the sinter plant, while the CASOH technology is employed to process blast furnace gas and basic oxygen furnace gas, acting as a pre-combustion carbon capture solution. CASOH produces an H₂-rich mixture, which is utilized internally to generate steam. It is worth to underline that when H₂ is available in the steelmaking process it could be used as reducing agent, although, in this case, a H₂-N₂ separation step must be included. The CO₂ captured by both DISPLACE and CASOH can either be stored or used in the production of other goods. This study was carried out within the context of the C⁴U project which aims to advance DISPLACE and CASOH from TRL 5 to 7. The project also includes extensive analyses of the economic, environmental, and business impacts of deploying CCUS in large-scale steel plants within the North Sea Port industrial cluster ("C4U website," n.d.).

The paper is organised as follows: Section 2 gives details on the methodology adopted for the techno-economic assessment of the C⁴U steel mill, describing the analysed plants, the modelling of the DISPLACE and CASOH technologies and their integration within a BF-BOF steel mill, as well as the assumption for the economic analysis and the KPIs; Section 3 shows the results; Section 4 gives the conclusions. Additional details about the methodology and the results are given in Appendix A and in Appendix B.

2 Method

The methodology used for the techno-economic assessment of the C⁴U steel mill is outlined in Figure 3. First, the base and reference BF-BOF steel plants, which served as the benchmarks for calculating key performance indicators (KPIs) were defined. Next, the layout of the C⁴U steel mill was established, selecting the carbon capture technologies (DISPLACE and CASOH) to be integrated and determining the composition and mass flow rate of the gas to be treated in the carbon capture sections. A different gas distribution within the steel plant was chosen compared to the base case, introducing oxy-fired units to facilitate the post-combustion CO₂ capture in the DISPLACE columns. Simulations of the oxy-fired hot stoves, oxy-fired reheating ovens, and sinter plant with gas recirculation were performed to calculate the mass flow rate and composition of the flue gas to be fed to the DISPLACE technology. These data were input for simulating DISPLACE performance, conducted by TNO, the technology owner, using a Matlab code that models the DISPLACE technology. Multiple simulations were run to identify optimal operating conditions, targeting a carbon capture ratio (CCR) of 90% and a CO₂ purity (CP) of 95% (dry) at operating temperatures of 300, 350 and 400 °C and pressures of 5, 6, 7, and 10 bar. The results were integrated into the Aspen Plus model of DISPLACE within the steel plant. Separate Aspen Plus models were created for each of the three cases: decarbonization of flue gas from oxy-fired hot stoves, oxy-fired reheating ovens, and sinter plant. These models were used to define the heat exchanger network to recover waste heat and minimize additional fuel use for the carbon capture process. The Aspen Plus models were used also to calculate the electricity consumption of equipment like compressors and pumps required to compress the flue gas to the DISPLACE working pressure or the CO₂ stream to transport and storage pressure conditions. TNO's simulations

also determined the size of the DISPLACE (column diameter and height), the number of columns per train, and the number of trains, which are essential for CAPEX estimation. KPIs typical of this analysis were computed for each case. The single-unit analysis helped determine the optimal working conditions for each case. Similarly, CASOH integration was performed and simulated in Aspen Plus permitting to find optimal operating condition of the CASOH technology and to carry out the techno-economic assessment of the C⁴U steel plant. It should be also underlined that, in this work, no extra purification systems of the CO₂ streams produced by the carbon capture sections is considered. Further details are given in the following sections.

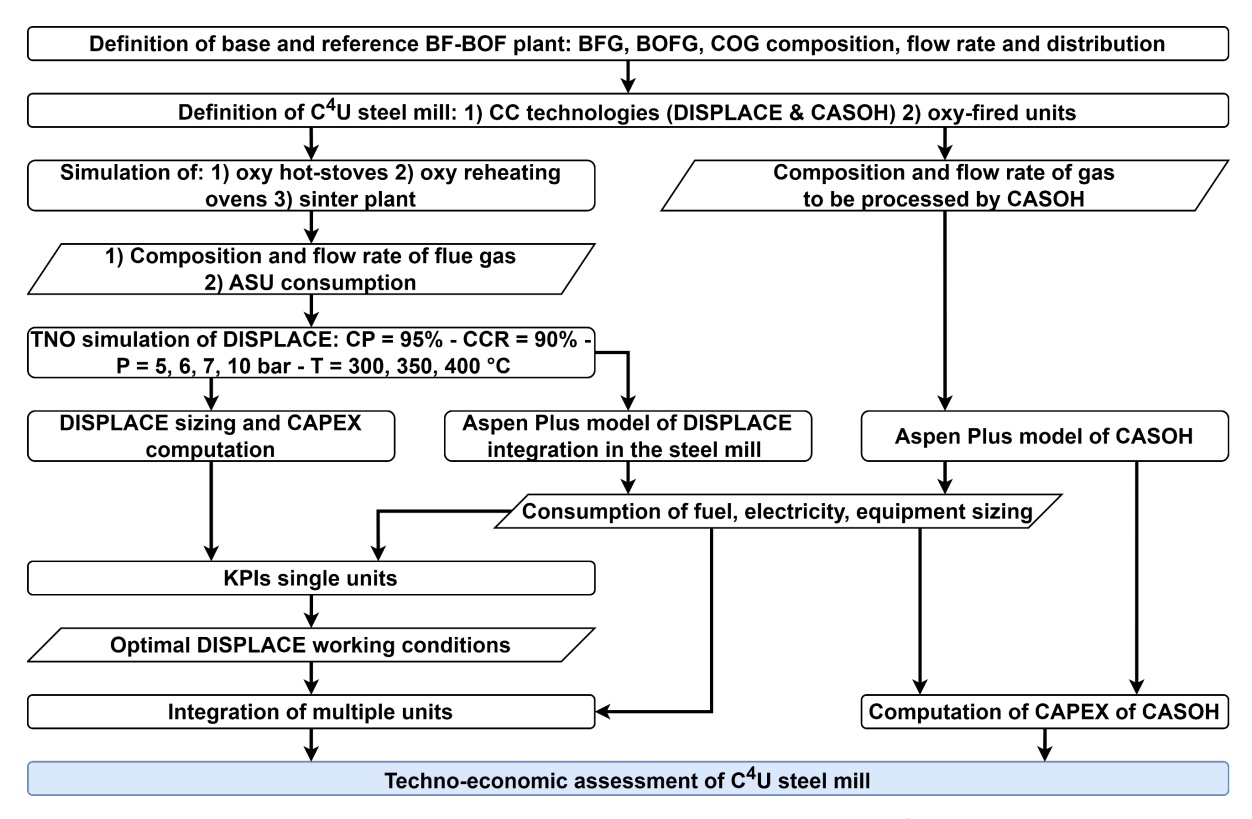


Figure 3: Methodology adopted for the techno-economic assessment of the C⁴U steel mill.

2.1 Analysed plants

The plants introduced in the description of the methodology are described in detail in the following sections.

2.1.1 Base BF-BOF plant

The base Blast Furnace-Basic Oxygen Furnace (BF-BOF) steel mill analysed in this study is modelled based on the plant described in (IEAGHG Technical Report, 2013), with modifications tailored to specific project needs, such as the plant size (in this study set at 3.16 Mt_{HRC}/y) and slight variations in the composition of BFG, as recommended within the C⁴U project consortium (Khallaghi et al., 2022). Table 2 provides details on the composition of BFG, BOFG, and COG. All sections of the steel plant have been meticulously modelled to ensure an accurate carbon balance across the entire facility.

Table 2: BFG, BOFG and COG composition.

Gas stream	Composition [% mol]										
Gas stream	CH ₄	CO	CO_2	H_2	H ₂ O	O_2	N_2				
BFG	-	21.79	20.54	2.30	4.00	-	51.36				
BOFG	-	56.92	14.44	2.64	12.16	-	13.84				
COG	23.24	3.87	0.97	60.05	3.15	0.19	5.82				

The definition of gas distribution within the base steel plant is pivotal for conducting the techno-economic assessment of integrating carbon capture technologies. This distribution governs the composition and mass flow rates of exhaust gases from various sections of the plant, which are crucial considerations for implementing post-combustion carbon capture technologies or for determining the flow rates of steel-making gases to be decarbonized (such as BFG, BOFG, COG) when employing pre-combustion carbon capture technologies.

2.1.2 Reference BF-BOF plant

In a steel plant there are numerous emission points that contribute to the overall emissions of the facility. Studies found in the literature typically focus on decarbonizing just one of these fluxes. Given that flue gas from the power plant accounts for about 50% of the total CO₂ emissions, decarbonization options for this gas stream are evaluated by (Khallaghi et al., 2022) and (Manzolini et al., 2022). The reference plants considered in this work integrate commercially ready carbon capture technologies, thus the methodology and plant layout presented by (Khallaghi et al., 2022) is adopted. The primary difference lies in the composition and mass flow rate of the gas being decarbonized; in this work, a mixture of blast furnace gas (BFG) and basic oxygen furnace gas (BOFG) is used as fuel in the power plant, whereas in (Khallaghi et al., 2022) only BFG is considered.

BFG and BOFG mixture is firstly compressed to 3 bar and then converted into H₂ + CO₂-rich gas in the WGS stage, reacting with steam. Steam, available at 3 bar and 145 °C, is heated to 330 °C and then introduced into the WGS reactor. The shifted gas is cooled to 355 °C to pre-heat the WGS feed mixture. Before entering the absorber column, the shifted gas is further cooled to 40 °C, and the condensed water is removed. In the absorber column, the syngas comes into contact with the lean solvent (MDEA) that absorbs the CO₂. A decarbonized clean fuel exits at the top of the column, while the CO₂-rich solvent exits from the bottom. The rich solvent is pumped to 6 bar and heated to 80 °C before entering the stripping column. The lean solvent leaves the bottom of the stripper, is expanded to 2 bar, cooled to 40 °C, and then fed to the top of the absorber. High-purity CO₂ exits the top of the stripper column, with evaporated water removed in a condenser. The CO₂-rich stream is then compressed to 78 bar in a multistage compressor, liquefied by cooling to 25 °C, and pumped to 110 bar. The simulation of the carbon capture plant has been carried out in Aspen Plus V14 and the ELECNRTL method has been selected, using the plant scheme shown in (Khallaghi et al., 2022) and the methodology described in (Zecca et al., 2023) as reference.

All the steam necessary for the WGS reaction is taken from the power plant's steam cycle at the exit of the medium-pressure steam turbine. Similarly, part of the steam used for solvent regeneration in the reboiler is sourced from the power plant. Therefore, the low-pressure steam turbine is not present in the steam cycle of the reference BF-BOF plant, as all the steam at the exit of the medium-pressure steam turbine is diverted to the carbon capture section. The condensate is then sent back to the heat recovery steam generator, reducing the electricity generated in the power plant. Additional steam has to be supplied to the reboiler, assumed to be generated in a natural gasfired boiler. The efficiency of the combined cycle, simulated in Aspen Plus V14, is 41.29%, generating 152.25 MW against a demand of 190.16 MW.

2.1.3 C^4U steel plant

In the C⁴U steel plant, two different technologies are integrated to reduce plant emissions. The DISPLACE technology is employed to decarbonize the flue gas from three units: the reheating ovens, hot-stoves, and the sinter plant, while the CASOH technology, a pre-combustion carbon capture technology, produces a hydrogen-rich stream from BF and BOF gases. As shown in Figure 4, a revised gas distribution has been proposed compared to the base steel plant (IEAGHG Technical Report, 2013). Various options were evaluated, considering the feasibility of adopting oxy-fired units like oxy-fired hot-stoves or oxy-fired reheating ovens. Oxy-fired units offer the advantage of generating more concentrated CO₂ in the flue gases, thereby facilitating the adsorption process in the DISPLACE columns. However, a drawback is the need for a larger air separation unit to produce the additional oxygen. These units use blast furnace gas as fuel instead of coke oven gas, possible because of the absence of a power plant. Consequently, all electricity for the C⁴U steel mill must be imported from the grid. CASOH technology provides the advantage of producing extra steam and a hydrogen-rich stream suitable for steam generation in the DISPLACE process. Several configurations involving single or multiple DISPLACE units were considered. Priority was given to using coke oven gas as the primary fuel source to fulfil the additional heat requirements for the DISPLACE carbon capture process, while exporting the H₂-rich stream from CASOH. If

COG proves insufficient to meet the DISPLACE heat demand, the hydrogen-rich stream serves as additional fuel, with any excess being exported.

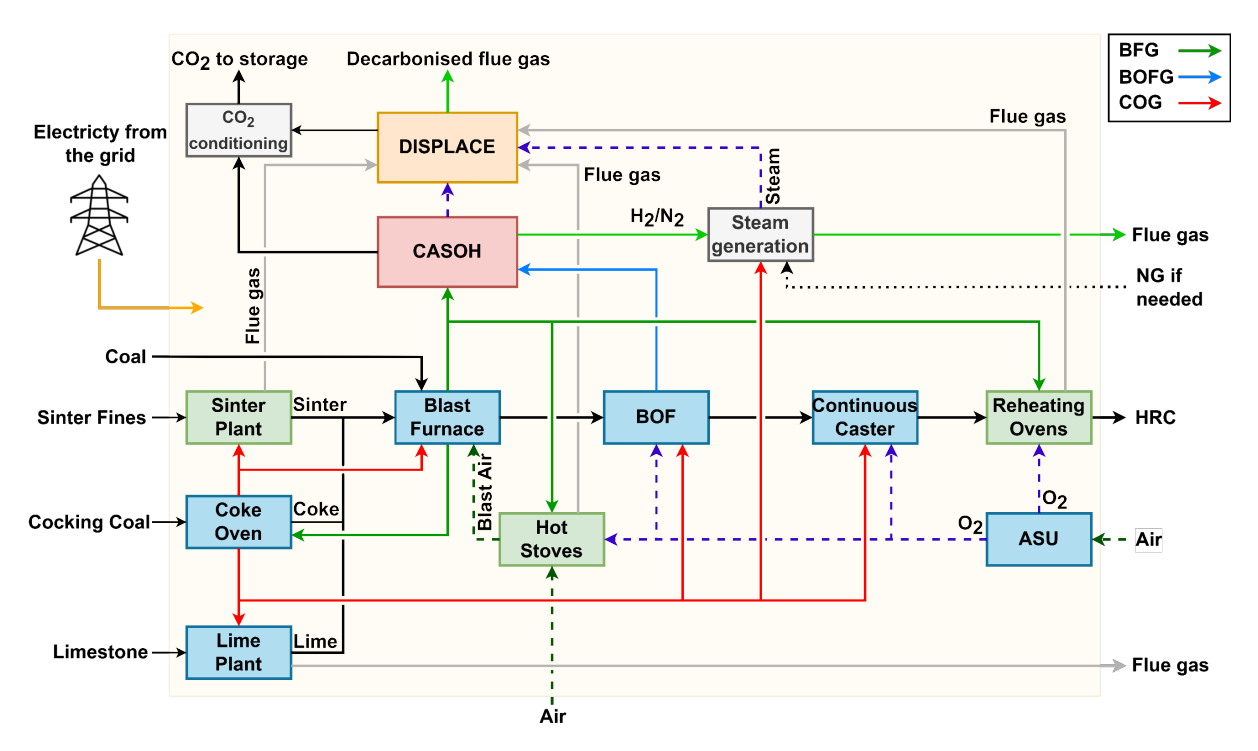


Figure 4: C⁴U steel plant simplified layout.

2.2 DISPLACE modelling and process integration

In a traditional BF-BOF steel mill, iron-bearing materials such as iron ore lump, sinter, and pellets undergo reduction in the blast furnace. These materials, along with additives like limestone and reducing agents such as coke, are introduced from the top of the furnace. Additionally, hot blast air enriched with oxygen is injected into the furnace's lower section, promoting the formation of carbon monoxide from coke, which subsequently reduces the iron ores to metallic iron (Remus et al., 2013). Hot stoves function as high-temperature heat exchangers that heat cold ambient air to a required temperature (900–1350°C) through a cyclical process. Typically, a combination of blast furnace gas and coke oven gas serves as fuel to generate hot combustion gases. These gases circulate through a network of heat-resistant refractory pipes and chambers until the materials reach the necessary temperature (1100–1500°C). At this point, the combustion gases are cut off, and cold ambient air is introduced in the opposite direction. The heat stored in the refractory bricks is transferred to the incoming air. This cycle repeats until the blast air reaches the target temperature, triggering the start of a new cycle (Remus et al., 2013). As part of the C⁴U project, the implementation of oxy-fired hot stoves has been proposed. In this approach, only BFG is used as fuel, and it is combusted with oxygen instead of air. This modification reduces BFG consumption while increasing CO₂ concentration in the flue gases, thereby enhancing the efficiency of the carbon capture process.

The performance of blast furnaces is enhanced by the prior preparation of the burden in the sinter plant. Ironbearing materials, such as iron ores and recycled materials from downstream operations (coarse dust, sludge from blast furnace cleaning, mill scale, etc.), are agglomerated with additives (quartzite, olivine, limestone, lime) and fuels (coke breeze). This operation improves the mechanical and metallurgical properties of the burden, producing a product characterized by high porosity, stable chemical composition, and constant melting behaviour (Niel et al., 2022; Remus et al., 2013). The raw materials are first collected and prepared in precise quantities, then mixed in a rotary drum with water addition. This mixture is subsequently placed on top of a 30 – 50 mm layer of recycled sinter on a large traveling grate. At the beginning of the grate, the sintering reaction is initiated by burners that ignite the coke breeze. Process air is drawn by blowers into distribution chambers, known as windboxes, located underneath the grate. At the end of the grate, the produced sinter is crushed, cooled, and divided into three fractions. The sinter fines are recirculated, the second fraction is used as a hearth layer, and the remaining part is

used in the blast furnace (Niel et al., 2022; Remus et al., 2013). Exhaust gas from the sinter plant represents a significant share of the emissions of the entire steel mill, accounting for about 14% of the base BF-BOF steel plant emissions. These gases also contain compounds such as heavy metals (particularly iron and lead compounds), alkali chlorides, sulphur oxides, NO_x, hydrogen chloride, hydrogen fluoride, hydrocarbons, polycyclic aromatic hydrocarbons (PAHs), and aromatic compounds. Being the aforementioned pollutants present in the order of magnitude of ppm they are not considered in this work. The typical composition of flue gas from the sinter plant is taken from (IEAGHG Technical Report, 2013). The CO₂ molar fraction is typically low, around 5%. This level is too low for efficient CO₂ capture in the DISPLACE columns, so a recirculation of the waste gas is proposed. Consequently, the composition of the exhaust gas from the sinter plant was computed with the objective of reducing the oxygen molar fraction to 4%, resulting in a CO₂ molar fraction above 16% (Table 3).

Reheating furnaces are used in hot rolling mills to heat steel stock (billets, blooms, or slabs) to approximately 1200 °C, a temperature suitable for the plastic deformation of steel, facilitating rolling in the mill. In the base steel mill, COG is used as fuel to heat the slabs in the walking beam furnaces. Within the C⁴U project, the adoption of oxy-fired reheating ovens has been proposed. In this scenario, BFG is used as fuel and burned with oxygen instead of air. Similar to the oxy-fired hot stoves, this increases the concentration of CO₂ in the flue gases, effectively enhancing the carbon capture process.

The optimal incorporation of DISPLACE technology into the steel mill layout has been carried out considering diverse operating conditions in terms of temperature (300, 350 and 400 °C) and pressure (between 5 –10 bar) (Zecca et al., 2025). The focus was on scenarios where carbon capture exceeds 90%, ensuring a minimum carbon purity of 95%. Through comprehensive simulations of the DISPLACE cycles, key parameters, including the number of columns, size dimensions, and steam consumption, have been accurately computed.

The lay-out of the DISPLACE integration for the decarbonisation of the reheating oven flue gases is reported in Figure 5. In the case of flue gas from hot-stoves and sinter plant a similar but less complex scheme was adopted (Zecca et al., 2025). This is due to the different temperature at which the flue gases are available. The flue gases, which composition is reported in Table 3, are typically slightly above atmospheric pressure. Before compression, they are cooled to 35 °C to minimize compression work, also contributing to pre-heat a portion of the water used for generating steam (utilized in the DISPLACE columns) up to 102 °C. In the case of flue gas from reheating ovens, the high temperature (500 °C) permits to generate part of the steam necessary for the carbon capture process. Similarly, the outlet gas streams from the DISPLACE process, the CO₂-rich stream and the CO₂-lean gas stream, are cooled, generating steam. A furnace is employed to supply heat to the gas stream exiting the compressor and to superheat the steam to the DISPLACE working temperature. This furnace can alternately use natural gas, coke oven gas or the H₂-rich stream from CASOH as fuels. Prior to entering the furnace, the fuel and combustion air are preheated by the furnace flue gases. To prevent the presence of non-condensable species in the steam, a deaerator is included. The CO₂-rich stream is brought to the conditions for transport and storage through a multistage compressor, reaching pressures of up to 78 bar, then being liquefied at 25 °C and finally pumped to a pressure of 110 bar as described in (Wright et al., 2011; Zecca et al., 2023).

Simulations of DISPLACE integration were performed using Aspen Plus 14 using the RKS-BM property method starting from a detailed DISPLACE model developed by TNO and described in (Zecca et al., 2025).

Table 3: Flue gas streams processed by DISPLACE with corresponding thermodynamic conditions.

El	ṁ	Т	P [bar]	Composition [%vol]					
Flue gas	[kg/s]	[°C]		CO ₂	CO	O_2	N_2	Ar	H_2O
Reheating ovens	78.66	500	1.03	41.90	-	1.00	50.81	0.04	6.25
Hot-stoves	87.88	140	1.03	41.90	-	1.00	50.81	0.04	6.25
Sinter plant	123.99	120	1.03	16.84	0.32	4.00	64.15	-	14.69

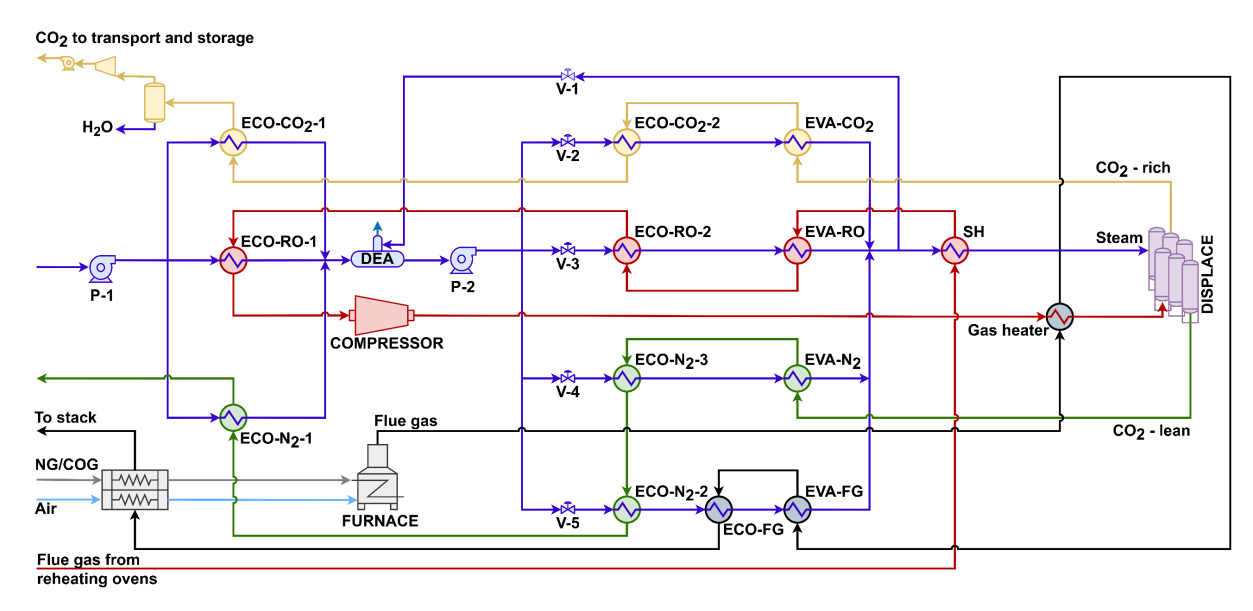


Figure 5: Plant scheme of the integration of DISPLACE technology for decarbonisation of flue gas from reheating ovens.

2.3 CASOH modelling and process integration

CASOH process flow diagram is shown Figure 6. A mixture of blast furnace gas and basic oxygen furnace gas is transformed into a H₂-rich stream through five primary steps (i.e., CASOH reaction, calcination, oxidation, purge and reduction) conducted in multiple packed-bed reactors operating in parallel. These reactors dynamically alternate between different temperatures and pressures to suit each step's requirements (Fernández et al., 2020).

In the CASOH step, the gas mixture is compressed to 10 bar and mixed with steam, maintaining a steam-to-CO ratio of 2. Before entering the CASOH reactor, the gas mixture is heated to around 520 °C in a furnace by burning a fraction of the H₂-rich gas produced in the reactor. Inside the reactor, CO from the gas mixture undergoes the water-gas shift reaction, catalysed by Cu-based particles, producing H₂ and CO₂. Simultaneously, CaO sorbent reacts with both the generated CO₂ and the CO₂ initially present in the gas through carbonation, forming CaCO₃. This carbonation shifts the equilibrium toward increased H₂ production by continuously removing CO₂ from the gas phase, achieving a high CO conversion (99%) and yielding a gas stream rich in H₂ (around 30% by volume). The exothermic reactions of WGS and carbonation raise the bed's temperature to around 750 °C. The gas stream is cooled down to 210 °C with saturated water at 12 bar and 190 °C, generating MP steam.

In the calcination step, the reactor bed is depressurised under mild vacuum conditions (0.5 bar) and high-temperature steam (525 °C and 3 bar) is fed into the reactor. The heat generated from the WGS and carbonation reactions provides most of the heat required for the calcination, and the remaining is provided by burning a fraction of the H₂-rich gas in a furnace. The reactor bed temperature increases to 833 °C and the outlet gas stream is cooled down to 210 °C with saturated water at 12 bar and 190 °C, generating MP steam. A high-purity CO₂ stream (over 99% by mol) is released via CaCO₃ calcination and water condensation.

In the oxidation step, air is introduced into the reactor and reacts with the metal-based particles (primarily Cu), oxidizing them to CuO. The exothermic reaction rapidly increases the bed temperature to around 600 °C, ensuring fast and complete O₂ conversion. High pressure (10 bar) and moderate temperatures minimize CO₂ release from any partial calcination of CaCO₃. The product gas is mainly N₂ (over 99% by mol) and the stream is cooled down to 210 °C with saturated water at 12 bar and 190 °C, generating MP steam.

After oxidation, a purge step is implemented using an inert gas (N_2) . The inert gas enters the reactor at approximately 10 bar and 190 °C and sweeps the oxygen gas remaining in the reactor as it flows through the bed. This process prepares the reactor for the next stage and allows for the recovery of high-temperature heat, as the gas outlet is cooled from 603 °C to 210 °C with saturated water at 12 bar and 190 °C.

Finally, in the reduction step, around 15% of the H₂-rich stream from the CASOH reaction is used to regenerate the CaO sorbent by calcining CaCO₃ back to CaO at 8.5 bar. Also, H₂ reacts with CuO, converting it back to Cu. The use of the H₂-rich stream as the reducing gas avoids consuming higher calorific value gases and eliminates

the need for an external heat source, as the exothermic reactions provide the necessary energy (Fernández et al., 2020). The outlet gas is cooled down to 210 °C with saturated water at 12 bar and 190 °C, generating MP steam.

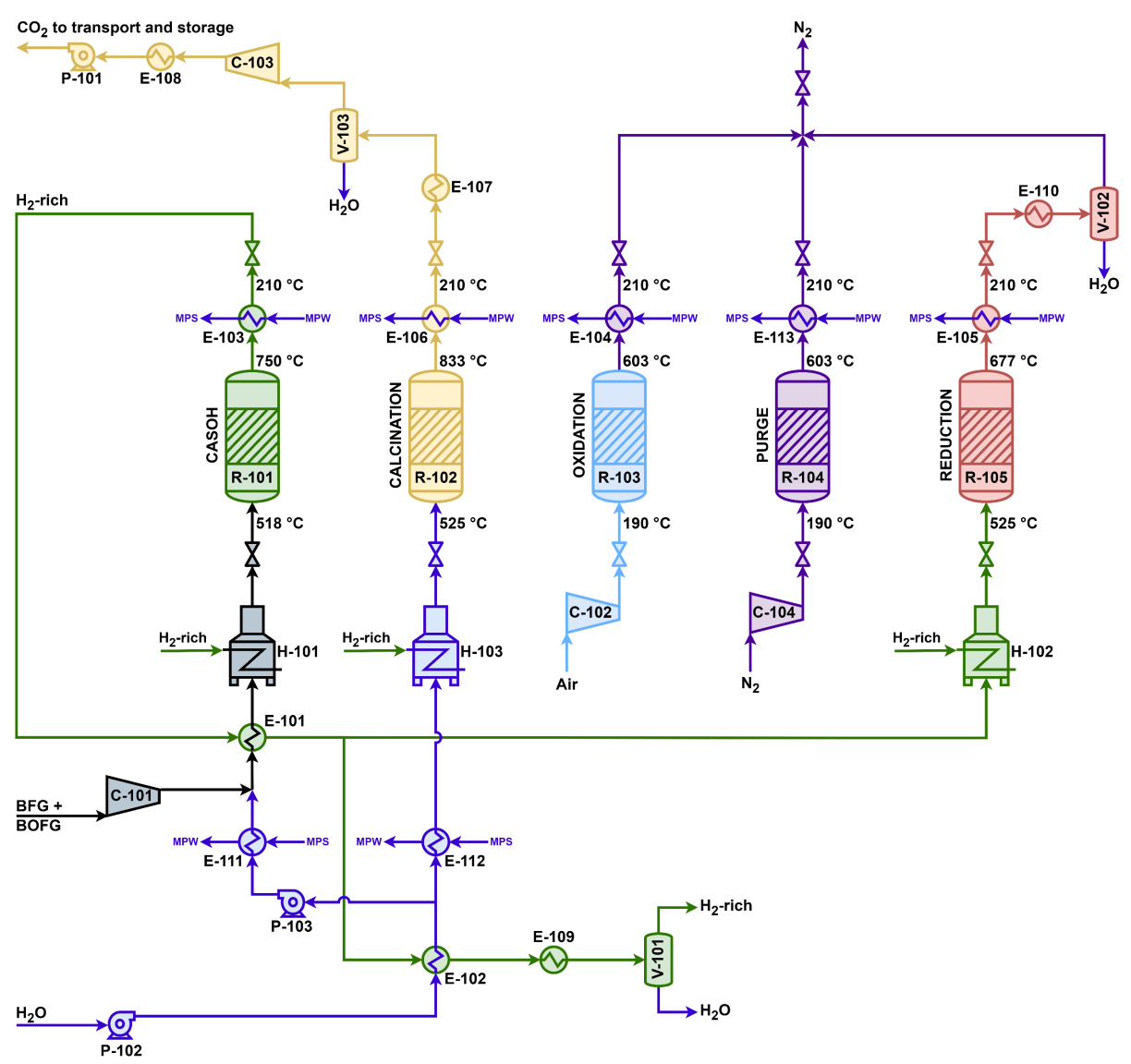


Figure 6: Process flow diagram of the CASOH process.

The five reaction stages of the CASOH process were modelled with a 1-D reactor model that integrates mass transfer limitations, energy balances and kinetics of the gas-solid reactions (Abbas et al., 2021). The model predicts the molar composition of the product gases at the outlet of the packed-bed reactor and the maximum temperature achieved in each stage. These values are used as inputs in Aspen Plus to replicate the CASOH process using a 0-D model of a continuous process, even though the process is dynamic. Table 4 shows the operating conditions of the CASOH stages.

Table 4: Operating conditions of CASOH reaction stages used in the process modelling.

Stage	Pressure (bar)	Temperature (°C)
CASOH	9.7	750
Calcination	0.5	833
Oxidation	10	603
Purge	9.5	603
Reduction	8.5	677

2.4 Other components modelling

This sections summarizes the methodology used for the modelling of the plants aforementioned. Table 5 details the property methods selected for each case, along with the Aspen Plus unit operation blocks for the primary equipment in each plant. Additional minor equipment, such as mixers, splitters, valves, reactors, pumps, compressors, and heat exchangers, are also utilized in the plant simulations.

Table 5: Property methods and Aspen Plus components used in the process modelling.

Plant section	Aspen Plus ID	Comments / Specifications						
DISPLACE - (RKS-BM pro	operty method)							
DISPLACE	Sep	A calculator block computes the mass flow rate and composition of the outlet streams						
Flue gas compressor	MCompr	2 stage; $\eta_{p,1,2} = 0.8$; $\eta_m = 0.95$; $T_{\text{intercooling}} = 50 ^{\circ}\text{C}$						
Deaerator	Flash2							
Furnace	RGibbs							
Gas-gas heat exchanger	HeatX	Minimum ΔT gas-gas heat exchanger = 15 °C						
Pumps	Pump	$\eta_h = 0.75; \eta_m = 0.95$						
CASOH - (PENG-ROB property method)								
CASOH reactor	RStoic + RGibbs	RStoic used to define 99% conversion of CO to CO ₂ and H ₂ ; RGibbs used to calculate phase and chemical equilibrium in the reactor products						
Calcination reactor	Heater	Temperature 833 °C						
Oxidation reactor	Heater	Temperature 603 °C						
Reduction reactor	RStoic	Fractional conversion 100% of CO and H ₂ to CO ₂ and H ₂ O						
BFG + BOGF compressor	MCompr	3 stages; p _{out} = 10.8 bar; $\eta_{p,1,2,3}$ = 0.75; η_m = 0.95; T _{intercooling} = 30 °C; Δ p _{intercooler,1,2} = 0 bar						
Air compressor	MCompr	2 stages; p _{out} = 10.6 bar; $\eta_{p,1,2}$ = 0.75; η_m = 0.95; T _{intercooling} = 30 °C; Δ p _{intercooler,1} = 0 bar						
N ₂ compressor	MCompr	2 stages; p _{out} = 9.5 bar; $\eta_{p,1,2}$ = 0.75; η_m = 0.95; T _{intercooling} = 40 °C; Δ p _{intercooler,1} = 0 bar						
Furnaces	Heater	A fraction of the H ₂ -rich gas from CASOH-reactor is burned						
Pumps	Pump	$\eta_h = 0.75; \eta_m = 0.95$						
Reactor outlet coolers	Heater	Cooling fluid: saturated water at 12 bar and 190 °C; MP steam is generated						
CO ₂ compression train - (R	KS-BM property r	nethod)						
CO ₂ compressor	MCompr	3 stages; p _{out} = 80 bar; $\eta_{p,1,2} = 0.8$; $\eta_{p,3} = 0.75$; $\eta_m = 0.95$; T _{intercooling} = 28 °C; Δ p _{intercooler,1} = 0.05 bar; Δ p _{intercooler,2} = 0.19 bar						
CO ₂ pump	Pump	Discharge pressure = 110 bar; $\eta_h = 0.75$; $\eta_m = 0.95$						
MDEA CC capture sections	- (ELECNRTL pi	roperty method)						
WGS	RGibbs	p = 3 bar; duty = 0; calculate phase equilibrium and chemical equilibrium						
Absorber	RadFraq	Equilibrium; 20 stages; condenser: none; reboiler: none						
Stripper	RadFraq	Equilibrium; 20 stages; condenser: partial-vapor-liquid; reboiler: Kettle						
Regenerative heat exchanger	HeatX	Pinch point $\Delta T = 10^{\circ} C$						
Pump	Pump	Discharge pressure = 6 bar; $\eta_h = 0.75$; $\eta_m = 0.95$						
Expander	Compr	Discharge pressure = 110 bar; $\eta_{is} = 0.85$; $\eta_m = 0.95$						
Waste heat recovery - (STE	AMNBS property	method on water/steam side)						
Economiser; evaporator; superheater	HeatX	Minimum ΔT gas-liquid heat exchanger = 10 °C; economizer ΔT subcooling = 5 °C; economizer hot-side pressure drop = 0.2 bar; economizer cold-side pressure drop = 0.7 bar; evaporator hot-side pressure drop = 0.2 bar						

2.5 General assumptions

General assumption used in the techno-economic assessment and common to all the plants analysed are shown in Table 6.

Table 6: Assumptions for the thermodynamic assessment.

Parameter	Unit	Value
Steel plant capacity	Mt _{HRC} /y	3.16
Plant availability	h/y	8200
NG LHV	MJ/kg	46.87
COG LHV	MJ/kg	40.21
Electricity CO ₂ emissions	$kg_{\rm CO2}\!/\!MWh_{el}$	250
Water recovery from CO ₂ stream	%	90

2.6 Methodology for the economic assessment

This section summarizes the key assumptions used to perform the economic assessment. The methodology adopted to calculate the capital costs is based on bottom-up approach starting from the Total Equipment Costs (TEC) and computing the Total Annual Cost (TAC) as previously described in (Khallaghi et al., 2022; Manzolini et al., 2020; Zecca et al., 2023). The CEPCI index, computed as the average between the years 2019 and 2022 (equal to 712.47) was used to update the cost of equipment found in literature. Table 8 summarizes the updated reference cost of equipment used to carry out the economic assessment. Table 7 lists the general assumptions that are common across all cases evaluated. Electricity and natural gas prices are crucial factors influencing operational costs. The prices used in the assessment were derived from data reported in ("International industrial energy prices - GOV.UK," n.d.), reflecting average values for the European Union between 2019 and 2022. Specifically, annual industrial electricity prices, inclusive of environmental taxes and levies for very large consumers, were considered. Similarly, annual industrial natural gas prices, including taxes for large consumers, were used.

Table 7: Assumptions common to all plants for the economic assessment.

Parameter	Unit	Value
Currency exchange	€/\$	0.92
NG/BFG/BOFG/COG buying/selling price	€/MWh _{LHV}	50
Electricity price	€/MWh _{el}	125
Electricity selling price	€/MWh _{el}	1/3·El. price
Discount rate	%	8.00
Lifetime	years	25
Fixed Charge Factor	%	9.37
Water cost	€/m³	1
Personnel annual salary	€/y	60000
Total Installation Cost	% TEC	104
Indirect Costs	% (TEC+TIC)	14
Contingency	% (TEC+TIC+IC)	10
Owner's Costs	% (TEC+TIC+IC)	5
CO ₂ transport and storage	€/t _{CO2}	40
CO ₂ tax	€/t _{CO2}	0
N° additional employees per CC section	-	15
Maintenance cost for CO ₂ capture section in BF-BOF plant	% TPC _{CC section}	2.5
DISPLACE maintenance costs	% TPC _{DISPLACE CC} ·FCF	5

Table 8: Equipment reference cost.

Component	Scaling parameter	$C_0 [M \epsilon]$ S_0 f		f	Reference
CO ₂ capture unit (MDEA)	CO ₂ mass flow rate [t/h]	10.52	12.4	0.60	(Cormos et al., 2020b)
CO ₂ compressor and condenser	Power [MW]	55.24	50.5	0.67	(Manzolini et al., 2020)
Furnace	Heat duty [MW]	0.30	1.00	1.00	(Khallaghi et al., 2022)
Compressor	Power [MW]	10.17	15.3	0.67	(Manzolini et al., 2020)
Pump	Volumetric flow [m³/h]	0.28	250	0.14	(Huijgen et al., 2007)
WGS	H ₂ and CO flow rate [kmol/s]	3.89	1.68	0.67	(Manzolini et al., 2020)
Steam turbine	Power [MW]	41.43	200	0.67	(Manzolini et al., 2020)
Heat exchanger	Heat transfer [MW]	16.25	138	0.67	(Guo et al., 2014)

The cost of CO_2 transport and storage for this study is set at $40 \text{ } \epsilon/t_{CO_2}$. This figure aligns with estimates provided by Smith et al., who suggest a range of 4 and 45 \$/t_{CO_2}\$ depending on factors such as transport distance, scale (i.e. quantity of CO_2 transported and stored), monitoring assumptions, reservoir geology and pipeline capital costs (Smith et al., 2021).

In the case of C⁴U steel mill, as detailed in section 2.3 the CASOH unit generates a H₂-rich stream and steam. Any surplus hydrogen is assumed to be sold at a price equivalent to the levelized cost of blue hydrogen (LCOH) produced via steam methane reforming. The National Energy Technology Laboratory (NETL) indicates the variation of LCOH with respect to natural gas price for NG prices ranging from 1 to 10 \$/MMBtu equivalent to 3.14 and 31.39 ϵ /MWh_{LHV} (Lewis et al., 2022). For the purposes of this study, the data were extrapolated to encompass NG prices up to 100 ϵ /MWh_{LHV} (or 31.86 \$/MMBtu). The relationship between hydrogen cost and NG price is represented by a linear equation derived from the plotted data, adjusted here for NG prices (C_{NG}) in ϵ /MWh_{LHV}:

$$LCOH \left[\text{€/kg}_{\text{H}_2} \right] = 0.7513 + 0.05373 \times C_{\text{NG}}$$
 (1)

In the context of the CASOH technology, the economic assessment was conducted based on data gathered from vendors during the C⁴U project. Data included the cost of the main process equipment (e.g., reactors, compressors, furnaces, heat exchangers, pumps) estimated based on the equipment size and material of construction. The base cost of equipment (for a reference size or capacity) was updated using a scaling factor of 0.7 and a reference property (e.g., duty for furnaces, power for compressors, etc.). The CASOH plant is designed to process the gas mixture (BFG + BOFG) in 4 trains. Each train has 16 reactors: 6 are used for the CASOH reaction, 6 for calcination, 1 for oxidation, 1 for reduction and 1 for purge. Each reactor has 5 valves at the inlet and the outlet, which are used to dynamically alternate between the different CASOH stages. The list of equipment and its cost are included in the Appendix B.

The methodology used for computing the total equipment cost of the DISPLACE units is described in (Zecca et al., 2025).

2.7 Key Performance Indicators

The comparison across all investigated cases is conducted using economic and environmental Key Performance Indicators (KPIs), commonly referenced in literature (Gentile et al., 2022; Khallaghi et al., 2022; Manzolini et al., 2020). The environmental indexes considered include the primary energy consumption (PEC), the specific CO₂ emissions (e_{CO2}), the CO₂ capture ratio (CCR), SPECCA and CO₂ avoidance (CA).

$$PEC\left[\frac{GJ_{LHV}}{t_{HRC}}\right] = \frac{\dot{m}_{fuel}LHV_{fuel} + PEC_{el} + \dot{Q}_{req}/\eta_{th}}{\dot{m}_{HRC}}$$
(2)

$$e_{\text{CO}_2} \left[\frac{t_{\text{CO}_2}}{t_{\text{HRC}}} \right] = \frac{\dot{m}_{\text{CO}_2}}{\dot{m}_{\text{HRC}}} \tag{3}$$

$$CCR \left[\%\right] = \frac{\left(\dot{m}_{CO_2}\right)_{CO_2 - product}}{\left(\dot{m}_{CO_2} + \dot{m}_{CO}\right)_{feed}} \cdot 100 \tag{4}$$

$$SPECCA \left[\frac{GJ_{LHV}}{t_{CO_2}} \right] = \frac{PEC_{capture} - PEC_{no\ capture}}{e_{CO_2,no\ capture} - e_{CO_2,capture}}$$
(5)

$$CA [\%] = \frac{e_{CO_2,\text{no capture}} - e_{CO_2,\text{capture}}}{e_{CO_2,\text{no capture}}} \cdot 100$$
(6)

In this study, the primary energy consumption (PEC) associated with electricity generation varies based on its carbon intensity. Values provided in Table 9 serve as reference points, with linear interpolation used for intermediate scenarios. In the renewable energy scenario, with a carbon intensity of 0 kg_{CO2}/MWh_{el}, implying no fossil fuel consumption during operation, the PEC related to electricity generation is considered as 0 MWh_{LHV}/MWh_{el}. When the electricity carbon intensity reaches 350 kg_{CO2}/MWh_{el}, it is assumed that the electricity is generated in a natural gas combined cycle (NGCC) plant with an efficiency of 60%.

Table 9: PEC of electricity generation.

Parameter	Unit	RES	NGCC
Electricity C.I.	$kg_{\rm CO2}/MWh_{el}$	0	350
Cycle efficiency	$MW_{el}\!/\!MW_{LHV}$	-	60
PEC electricity generation	$MWh_{LHV}\!/MWh_{el}$	0	1.67

The economic performance is assessed computing the levelized cost of hot rolled coil (LCOHRC) and the cost of CO₂ avoidance (CCA). The total annualized cost (TAC) is computed according to equation (7) using the methodology described in (Khallaghi et al., 2022; Manzolini et al., 2020; Zecca et al., 2023) starting from the computation of the total equipment cost.

$$TAC\left[\frac{M \in}{y}\right] = TPC \cdot FCF + C_{f,O\&M} + C_{v,O\&M} - Revenues$$
 (7)

$$LCOHRC\left[\frac{\epsilon}{t_{HRC}}\right] = \frac{TAC}{\dot{m}_{HRC} \cdot h_{eq}} \cdot 10^{6}$$
(8)

$$CCA\left[\frac{\epsilon}{t_{CO_2}}\right] = \frac{LCOHRC_{capture} - LCOHRC_{no capture}}{e_{CO_2,no capture} - e_{CO_2,capture}}$$
(9)

To ensure a fair comparison among all the plant configurations analysed in this study and to account for differences in the import and export of commodities, the following assumptions have been made. For electricity export, such as in the case of the base BF-BOF plant, reductions in emissions and primary energy consumption are considered. These reductions are calculated based on the specific scenario chosen for the carbon footprint of electricity generation, using the values outlined in Table 9. Similarly, when exporting gas streams like COG and H₂-rich mixture or steam, reductions in emissions and primary energy consumption are also taken into account by computing the equivalent amount of NG on energy basis, which is assumed to be the fuel being replaced. Exporting electricity effectively means that another user does not need to purchase the equivalent amount of electricity from the grid, which would have its own associated carbon footprint and primary energy consumption based on the electricity generation scenario considered. Likewise, exporting COG, hydrogen or steam means that the purchaser does not need to buy an equivalent amount of natural gas which, in this study, is considered the baseline fuel that would otherwise be consumed.

3 Results

In this section the performance of the CASOH and DISPLACE units as well as the results of the techno-economic assessment of the C^4U steel mill are shown.

3.1 DISPLACE performances

As mentioned in previous sections multiple simulations of DISPLACE units were performed, considering different values of DISPLACE operating temperature and pressure. In Table 10 the results regarding the optimal cases for the three considered application are shown.

Table 10: Electricity and fuel consumption of DISPLACE units.

	D	т	Flue gas	CO ₂	Total	Fuel	0	CCR	СР	
Case	r [bar]	[°C]	compression [MW _e]	$\begin{array}{c} compression \\ [MW_e] \end{array}$	electricity [MW _e]	consumption $[MW_{th}]$	$e_{CO2-no\ capt.}$ $[t_{CO2}/t_{HRC}]$	[%]	[%]	
Reheating ovens	5	400	23.20	10.19	33.39	58.26	0.397	90.38	95.41	
Hot-stoves	5	400	16.00	11.28	27.28	103.14	0.444	90.38	95.41	
Sinter plant	5	400	27.21	7.59	34.80	113.20	0.298	90.43	95.05	

3.2 CASOH performances

The performance of CASOH processing a mixture of BFG and BOFG are given in Table 11. These data were used for the techno-economic assessment of C⁴U steel mill as shown in section 3.3. The CASOH unit, produces a steam stream that can be used in the DISPLACE units, reducing the consumption of fuel for steam production.

Table 11: Thermodynamic performance of CASOH when simultaneously integrated with DISPLACE.

Parameter	Unit	No capture	CASOH
Total BFG + BOFG input	MW_{LHV}	226.9	226.9
Thermal energy output	MW_{LHV}	226.9	169.5
Cold gas efficiency	%	100.0	74.7
Net power consumption	MW_{el}	-	57.9
Heat requirement	$MW_{th} \\$	-	61.3
CO ₂ flow rate for storage	kg/s	-	51.6
CO ₂ purity for storage	%	-	99.8
CO ₂ emission	kg/s	56.5	4.8
CO ₂ capture efficiency	%	-	91.5
Specific CO ₂ emission	$kg_{\rm CO2}\!/GJ_{\rm LHV}$	248.8	28.4
Specific CO ₂ emission	$kg_{\rm CO2}/t_{\rm HRC}$	527.4	45.0
Steam produced	MW	-	31.4
H ₂ -rich mix produced	kg/s	-	34.7
H ₂ -rich mix used for heat requirement	kg/s	-	13.3
H ₂ -rich mix available	kg/s	-	21.4
H ₂ -rich mix LHV	MJ/kg	-	4.89
H ₂ -rich mix composition			
- CO	%vol	-	2.14
- CO ₂	%vol	-	3.00
- H ₂	%vol	-	35.84
- H ₂ O	%vol	-	0.45
- N ₂	%vol	-	58.57

3.3 Overall plant performance and emissions for different level of integration

This section presents the results of the C⁴U steel plant with the simultaneous integration of CASOH and DISPLACE technologies. Similar to the base case, the C⁴U steel mill consumes 4845 t/day of coking coal in the coke plant and 1473 t/day of PCI coal in the blast furnace. The plant's electricity requirements are met by importing electricity from the grid, as there is no on-site power plant.

Different integration scenarios are presented and compared to the base and reference BF-BOF plants, including the integration of CASOH technology alone and the addition of DISPLACE to single or multiple units. When DISPLACE is integrated alongside CASOH, the graphs only indicate the steel mill section(s) equipped with DISPLACE, denoted as "HS" for hot-stoves, "RO" for reheating ovens, and "SP" for the sinter plant. In addition, the adoption of oxy-fired units, specifically hot-stoves and reheating ovens, is considered only when DISPLACE technology is implemented to decarbonize the flue gas from these sections.

Oxy-fired units necessitate installing a larger air separation unit, which increases both electrical consumption and capital expenditure thus justifying its installation only in the case of concurrent integration of DISPLACE. However, oxy-fired units produce exhaust gas streams with higher CO₂ concentrations compared to conventional equipment, making the CO₂ capture process less energy-intensive. Furthermore, a larger ASU can increase revenues from the sale of argon, partially compensating the higher expenditures. CASOH process could potentially benefit from the use of oxygen in the blast furnace as well, generating a more concentrated H₂-rich stream.

For scenarios where oxy-fired hot-stoves or reheating ovens are not adopted, some coke oven gas must be used alongside blast furnace gas to ensure that sufficient thermal energy is transferred to the hot-blast air and slabs. To simulate these conditions, hot-stoves and reheating ovens have been modelled in Aspen Plus. In these simulations, air is used as the comburent instead of pure oxygen, with a mixture of BFG and COG as fuel. The mass flow rate of air has been calculated to achieve 1% oxygen in the exhaust gases. The results of these simulations are presented in Table 12.

The available coke oven gas, which is not already used as fuel within the steel plant, was prioritized as the primary fuel source to meet the additional heat requirements for the DISPLACE carbon capture process, while exporting the hydrogen-rich stream from CASOH. If the available COG is insufficient to cover the DISPLACE heat demand, the hydrogen-rich stream is utilized as an additional fuel, with any excess being exported. Conversely, the heat demand of the CASOH process is fulfilled by using part of the H₂-rich mixture as fuel.

Gas distribution within the steel plant when carbon capture process is simultaneously applied to flue gas from hot-stoves, reheating ovens and sinter plant, along with pre-combustion CASOH technology is shown Figure 7. Table 13 details the amount of COG and H₂-rich mix exported in the analysed cases. For the base and reference BF-BOF cases there is no export of COG or H₂-rich mix.

Table 12: COG consumption in non-oxy-fired units.

Fuel	Non-oxy-fired HS	Oxy-fired HS	Non-oxy-fired RO	Oxy-fired RO
BFG (dry) [kg/s]	77.22	77.22	69.12	69.12
COG (wet) [kg/s]	0.333	-	0.278	-

Table 13: Export of COG, H2-rich mix, Ar for the analysed cases.

Gas exported	CASOH	RO	HS	HS-RO	HS-RO-SP
COG [kg/t _{HRC}]	34.43	31.05	20.07	9.38	-
COG [kg/h]	13270	11964	7734	3616	-
H ₂ -rich mix [kg/t _{HRC}]	200.06	200.06	200.06	200.06	60.91
H ₂ -rich mix [kg/h]	77097	77097	77097	77097	23474
Ar [kg/t _{HRC}]	2.88	4.81	5.04	6.98	6.98
Ar [kg/h]	1109	1855	1943	2689	2689

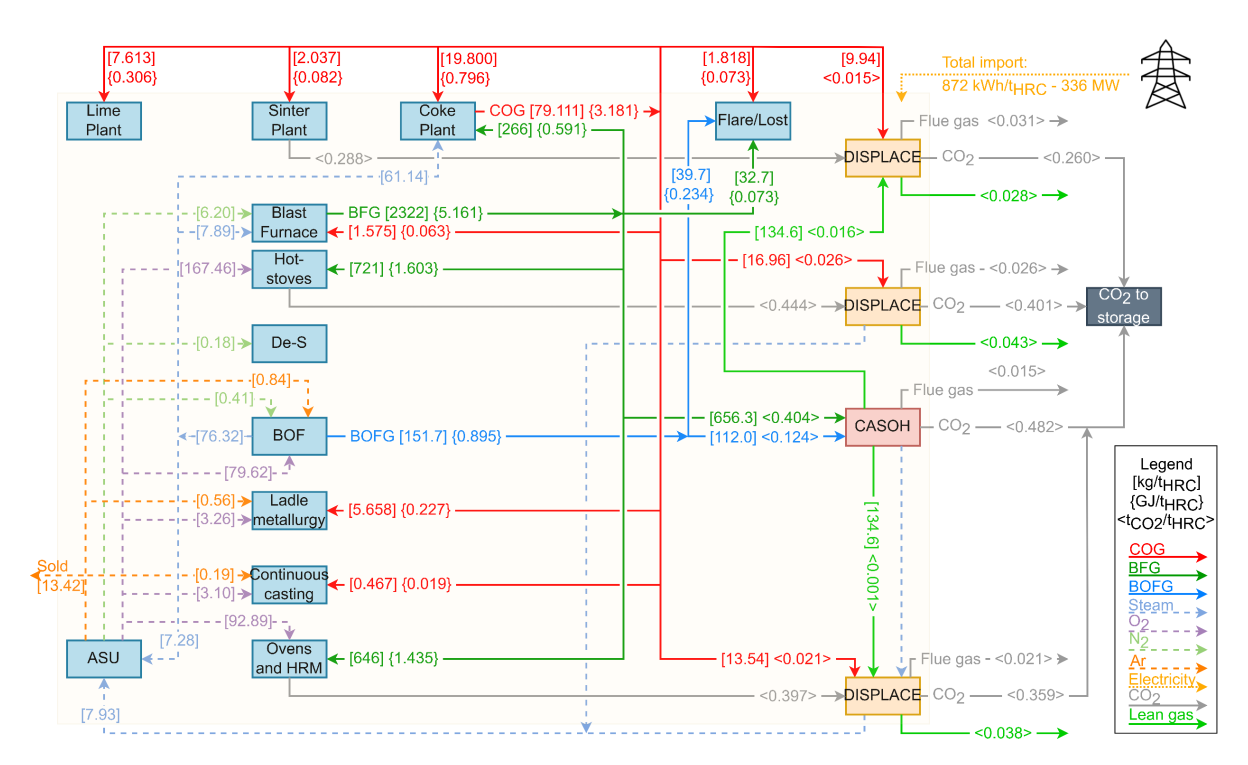


Figure 7: C⁴U steel plant layout. Gas distribution within the units.

The breakdown of CO_2 emissions for C^4U steel plant, considering various combinations of DISPLACE and CASOH implementation, is summarised in Table A.1. Figure 8 illustrates the CO_2 avoidance achievable with respect to the base BF-BOF plant, considering carbon intensities of imported electricity of 250 kg_{CO2}/MWh_{el} and 0 kg_{CO2}/MWh_{el}. A CO_2 avoidance equal to 72% can be reached in a renewable energy scenario.

Table A.2 presents the breakdown of primary energy consumption for the analysed C⁴U steel plant, while Figure 9 illustrates the SPECCA across different scenarios. The primary energy consumption related to COG and H₂-rich is calculated on the basis of the LHV and these values are negative in case of export from the plant. Interestingly, for the C⁴U steel plant, the positive factors of SPECCA are all associated with electricity imported from the grid or to the non-export of electricity. Therefore, in a renewable energy scenario where electricity is produced without fossil fuels consumption, and thus considering 0 GJ_{LHV}/MWh_{el} for the primary energy consumption associated to electricity generation, precisely because from renewable sources, the SPECCA results being negative. Conversely, in scenarios where fossil fuels contribute to electricity generation, the absence of a power cycle in the C⁴U plant significantly influences the SPECCA. The SPECCA related to the power consumption of CASOH is primarily due to the calcination process operating at 0.5 bar to produce nearly pure CO₂, which is subsequently compressed to 110 bar for transportation and storage. The electricity required for CO₂ compression is accounted for in all cases.

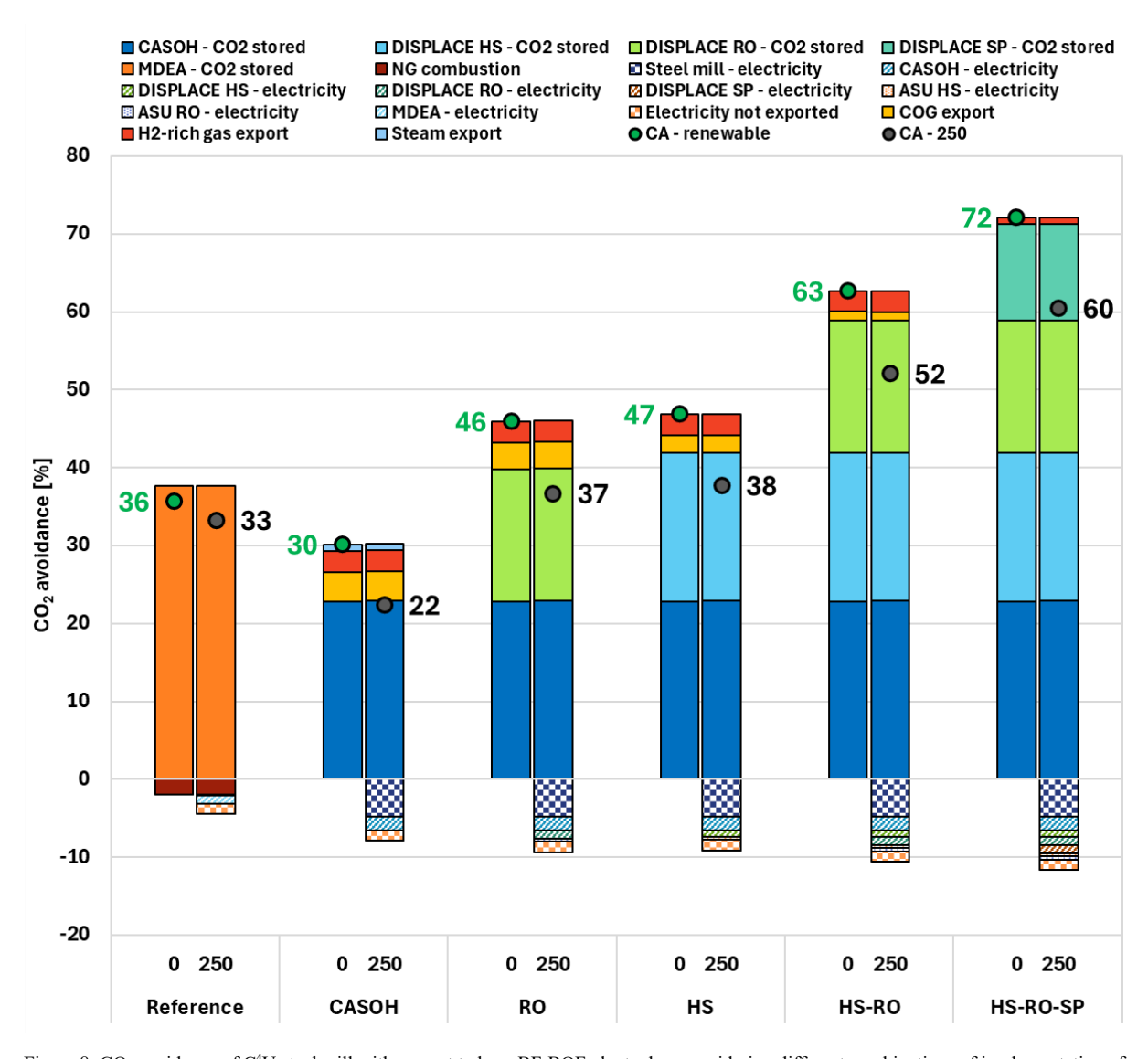


Figure 8: CO_2 avoidance of C^4U steel mill with respect to base BF-BOF plant when considering different combinations of implementation of DISPLACE and CASOH. The values in black and in green represent the CO_2 avoidance that can be achieved when considering a carbon intensity of imported electricity equal to 250 and 0 kg_{CO2}/MWh_{el} respectively.

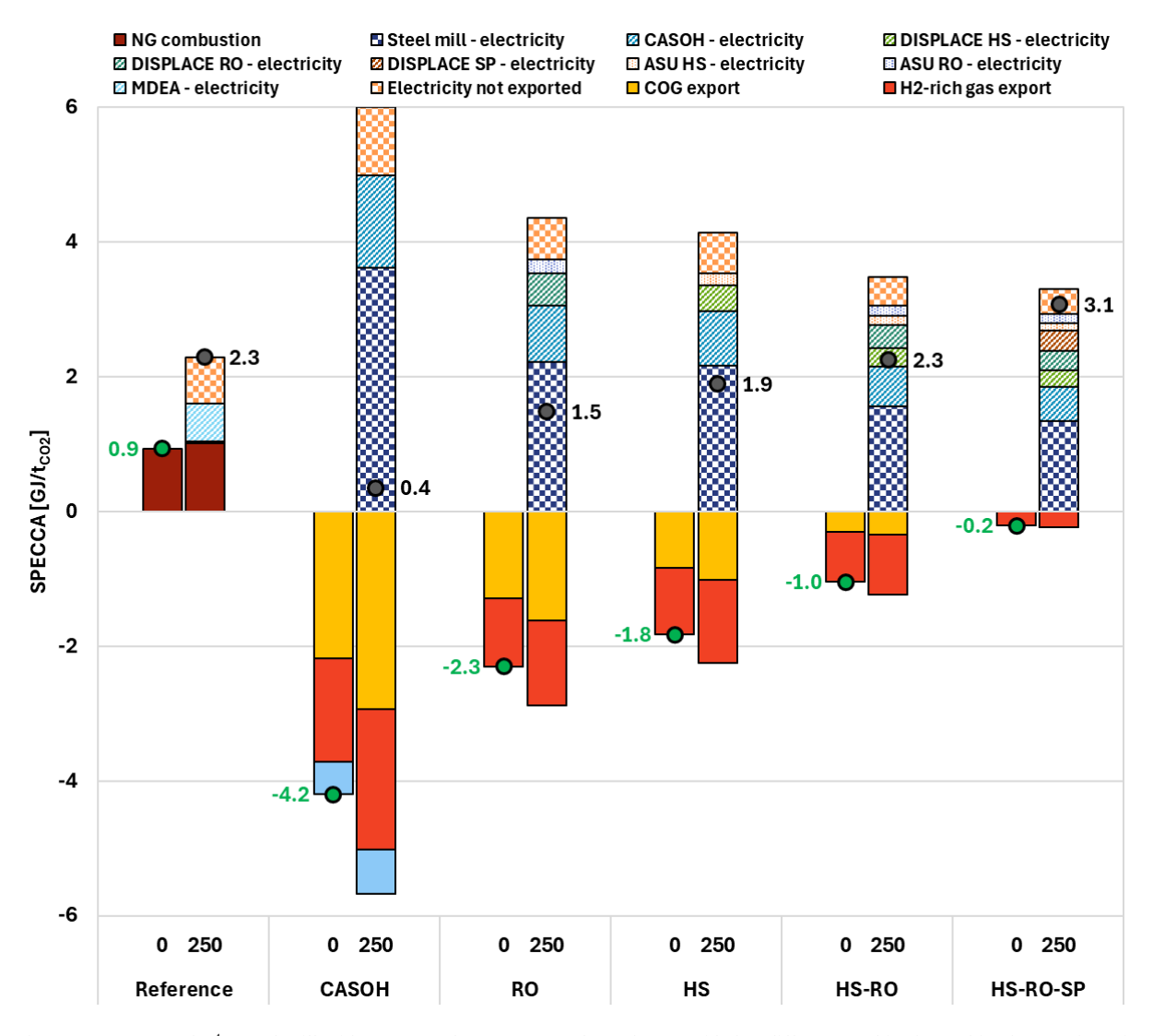


Figure 9: SPECCA of C⁴U steel mill with respect to base BF-BOF plant when considering different combinations of implementation of DISPLACE and CASOH. The values in black and in green represent the SPECCA considering a carbon intensity of imported electricity equal to 250 and 0 kg_{CO2}/MWh_{el} respectively.

Table 14 provides the breakdown of the levelized cost of hot rolled coil, with negative values indicating revenues. Further details are given in Table A.3. The levelized cost of hot rolled coil is 508.5 €/t_{HRC} for the base steel plant. This cost increases as carbon capture technologies are integrated, reaching 718.3 €/t_{HRC} at the highest level of CO_2 avoidance. Figure 10 displays the cost CO_2 avoided across different scenarios. The electricity not sold increases the CCA for all cases being electricity imported from the grid differently from the base BF-BOF plant, where electricity is exported and generates revenue. Many factors influence the CCA, including natural gas and electricity prices, as well as the carbon footprint of imported electricity. The carbon footprint of electricity directly impacts CO_2 avoidance and consequently the CCA. This has a bigger impact on the C^4U steel mill compared to the reference case, since all the electricity is imported from the grid. In the case of a higher price of natural gas the revenues from the sale of coke oven gas (COG) and hydrogen-nitrogen mixture (H₂-rich) increase, as their prices are linked to natural gas price, decreasing the CCA of the C^4U steel mill. The reference and CASOH cases present similar results in the renewable energy scenario, while the cost of CO_2 avoided increases when multiple point sources are decarbonised within the C^4U steel mill. In a renewable energy scenario, with a CO_2 of 72% the cost of CO_2 avoided is equal to 138 €/t_{CO2}.

Figure 11 shows the results in the case of availability of electricity at a price of $50 \, \text{e/MWh}_{el}$. As can be observed the reference case is less influenced by this parameter while the CCA of C⁴U stell mill sensibly decreases. In the renewable energy scenario, the CCA of the C⁴U is equal to $92 \, \text{e/t}_{CO2}$ with a CO₂ avoidance equal to 72% while the reference case shows a CCA of $85 \, \text{e/t}_{CO2}$ with a CO₂ avoidance limited to 36%.

Table 14: Breakdown of levelized cost of hot rolled coil for the analysed plants. All values are expressed in [€/t_{HRC}].

LCOHRC [ℓ/t_{HRC}]	Base	Ref.	CASOH	RO	HS	HS-RO	HS-RO-SP
CAPEX	118.7	133.6	141.8	151.7	152.3	162.0	170.6
- Steel mill	118.7	117.4	113.0	114.5	114.7	116.1	116.1
- CASOH	-	-	28.8	28.8	28.8	28.8	28.8
- DISPLACE	-	-	-	8.3	8.8	17.1	25.7
- MDEA	-	16.1	-	-	-	-	-
OPEX	406.0	460.7	489.8	519.8	519.0	549.0	570.7
- Electricity	-	12.3	68.9	84.5	82.0	97.7	108.9
- Natural gas	-	9.8	-	-	-	-	-
- Other OPEX	406.0	438.6	421.0	435.3	437.0	451.3	461.8
REVENUES	-16.2	-11.6	-61.1	-56.5	-50.6	-46.3	-23.0
- COG export	-	-	-19.2	-17.3	-11.2	-5.2	-
- H ₂ -rich mix export	-	-	-26.0	-26.0	-26.0	-26.0	-7.9
- Steam export	-	-	-4.3	-	-	-	-
- Other revenues	-16.2	-11.6	-11.6	-13.2	-13.4	-15.1	-15.1
Total	508.5	582.7	570.5	614.9	620.7	664.7	718.3

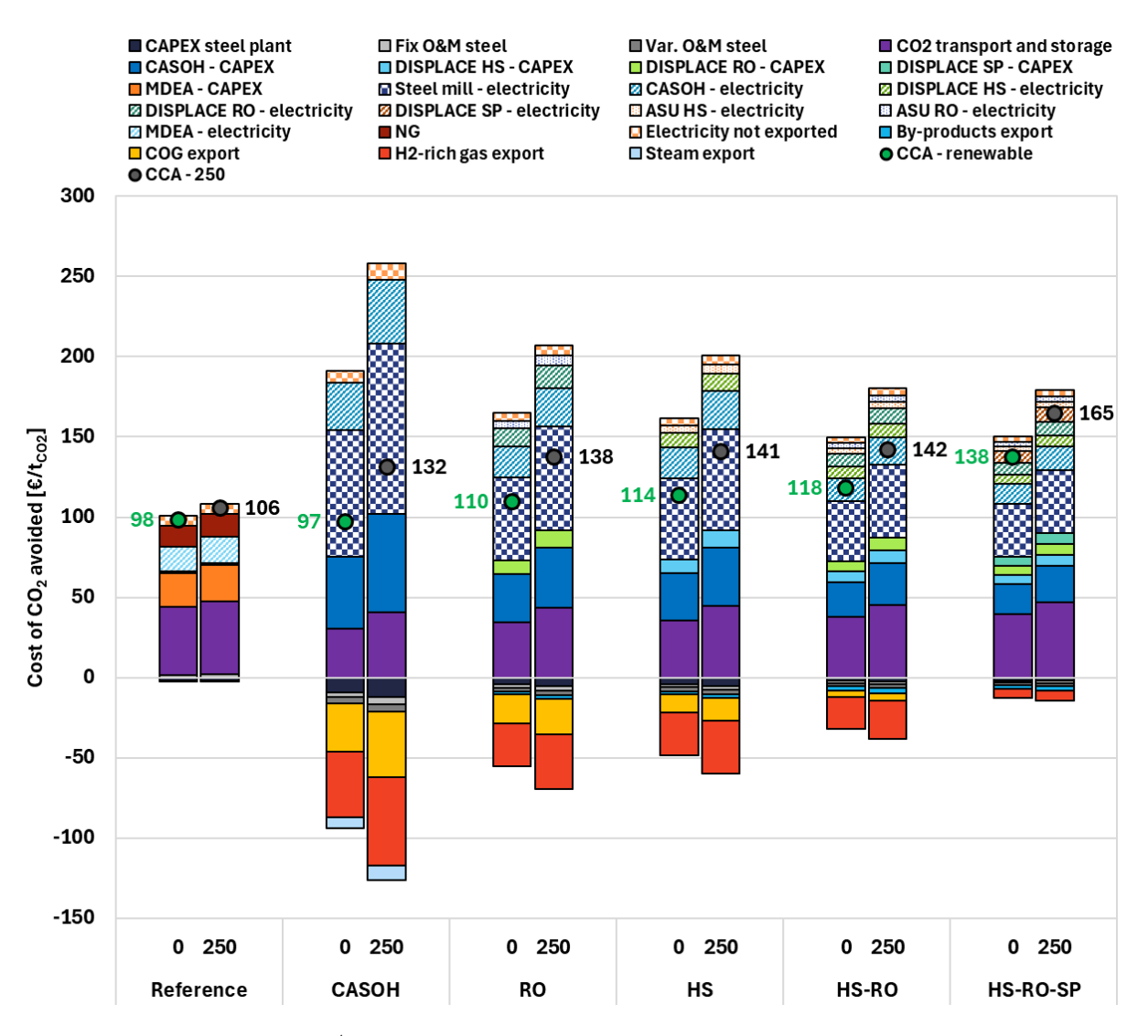


Figure 10: Cost of CO_2 avoided of C^4U steel mill with respect to base BF-BOF plant when considering different combinations of implementation of DISPLACE and CASOH. The values in black and in green represent the CCA considering a carbon intensity of imported electricity equal to 250 and 0 kg $_{CO2}$ /MWh $_{el}$ respectively.

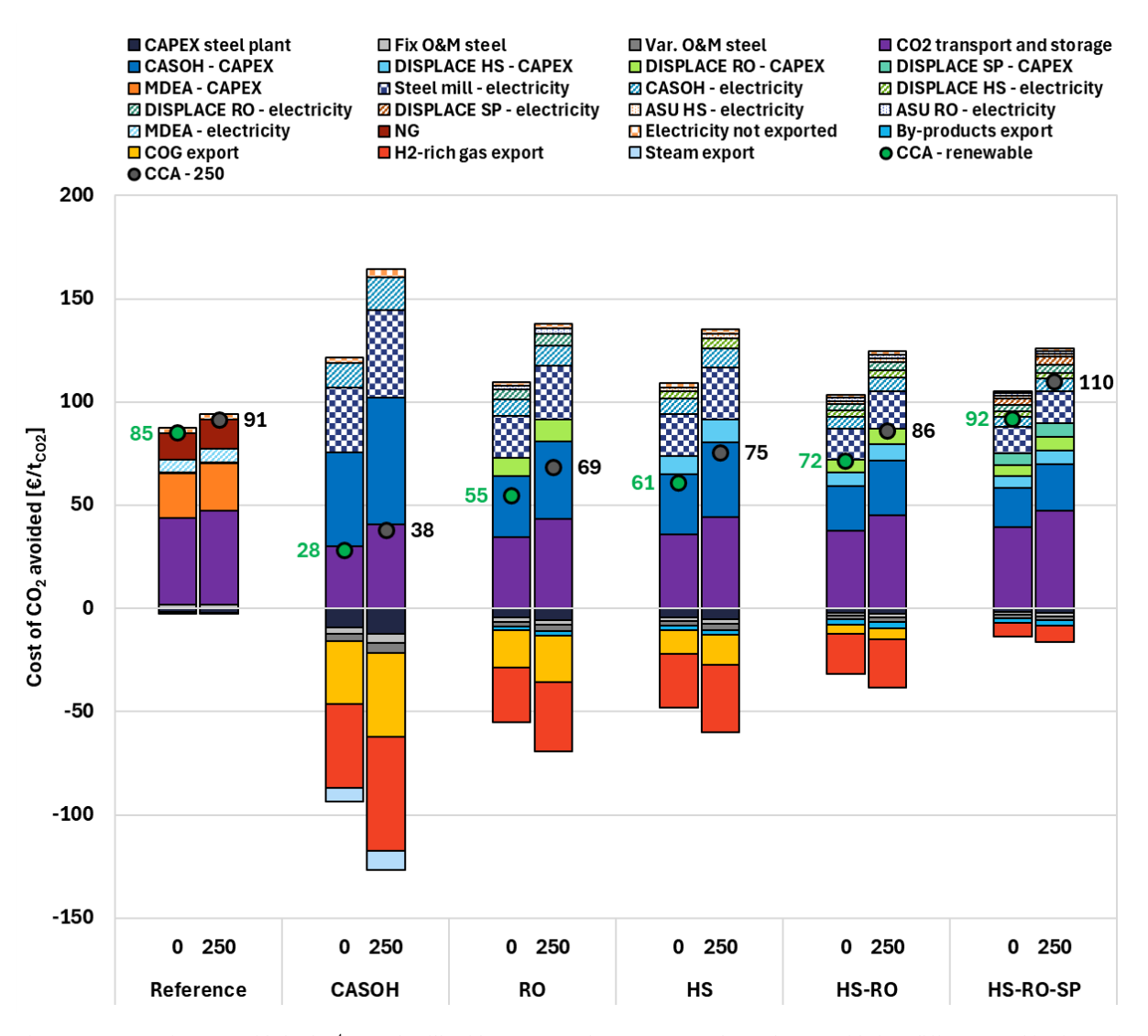


Figure 11: Cost of CO_2 avoided of C^4U steel mill with respect to base BF-BOF plant when considering different combinations of implementation of DISPLACE and CASOH. The values in black and in green represent the CCA considering a carbon intensity of imported electricity equal to 250 and 0 kg_{CO2}/MWh_{el} respectively. Electricity and natural gas prices set to 50 ϵ /MWh_{el} and 50 ϵ /MWh_{LHV} respectively.

4 Conclusions

Among the hard-to-abate sectors, steel industry is one of the major contributors to CO₂ emissions worldwide. In the long term, DRI process using green hydrogen is considered a good option, however, in the short term, alternatives must be explored. These alternative solutions must be integrated in BF-BOF steel plants and be capable of capturing CO₂ from multiple streams with different characteristics in energy content and CO₂ concentration. This work investigates two innovative CO₂ capture technologies developed and demonstrated at TRL 7 in the C⁴U project, named DISPLACE and CASOH, when integrated in a conventional BF-BOF steel mill to significantly reduce CO₂ emissions. CASOH processes a mixture of BFG and BOFG producing pure hydrogen and a concentrated CO₂ stream, while DISPLACE capture the CO₂ present in the exhaust gases coming from hot stoves, reheating ovens and sinter plant. Detailed analyses were conducted to optimize operational conditions for DISPLACE in various units, revealing its superiority over the benchmark MEA post-combustion technology under certain CO₂ concentration thresholds. Models of CASOH and DISPLACE where integrated in Aspen Plus V14 flowsheet to develop accurate heat and mass balances of the system as well component design for cost assessment. The two technologies, when simultaneously integrated, can achieve a CO₂ avoidance of 72% and a corresponding SPECCA of -0.2 GJ/t_{CO2} when green electricity is purchased from the grid. In the same scenario, the reference case shows a CO₂ avoidance of 36% and a SPECCA equal to 0.9 GJ/t_{CO2}. From an economic perspective, the

adoption of CO₂ capture technologies increases the cost of HRC to 718.3 $\[\in \]$ the which is 41% higher than the case without capture calculated assuming a cost of electricity and NG equal to 125 $\[\in \]$ /MWh_{el} and 50 $\[\in \]$ /MWh_{LHV}.

The cost of CO_2 avoided ranges between $138 \ ellectricity$ for the fully green and $165 \ ellectricity$ for electricity with 250 kg_{CO2}/MWh_{el} CO_2 emissions intensity. These values are higher than the corresponding one for the reference CO_2 capture technology considered, however doubling the CO_2 avoidance. It is worth to be underlined that the economic results are highly influenced by the prices of electricity and fuels. The techno-economic analysis, indeed, shows that in a scenario with low prices of electricity (i.e. $50 \ ellectricity$), the cost of CO_2 avoided of the C^4U steel mill reduces to $92 \ ellectricity$ in the case of renewable electricity, becoming closer to the CCA of the reference case. Further studies will investigate the utilization of H_2 with CO_2 for production of chemicals such as methanol and addressing additional flue gases as the one from lime plant to further increase the CO_2 avoided.

Acknowledgements

This paper is part of the C⁴U project that has received funding from the European Union's Horizon 2020 research and innovation programme under grant agreement N°884418.

The work reflects only the authors' views, and the European Union is not liable for any use that may be made of the information contained therein.

Appendix A

In this section, the detailed results of the analysed plants, specifically the breakdown of CO₂ emissions (Table A.1), of primary energy consumption (Table A.2) and of the levelized cost of hot rolled coil (Table A.3) are given.

Table A.1: Breakdown of CO_2 emissions for C^4U steel plants. All values are expressed in $[t_{CO2}/t_{HRC}]$ and negative values indicate CO_2 stored or related to fuel export. The results refer to the scenario in which the carbon intensity of electricity imported from the grid has a carbon footprint equal to $250~kg_{CO2}/MWh_{el.}$

CO ₂ emission [t _{CO2} /t _{HRC}]	Base	Ref.	CASOH	RO	HS	HS-RO	HS-RO-SP
Iron ore production	0.067	0.067	0.067	0.067	0.067	0.067	0.067
CO ₂ in steel mill	2.068	2.068	2.068	2.068	2.068	2.068	2.068
CO ₂ not treated	-	1.109	1.541	1.144	1.097	0.700	0.412
CO ₂ treated	-	0.959	0.527	0.924	0.971	1.368	1.656
CO ₂ to storage	-	-0.794	-0.482	-0.841	-0.883	-1.242	-1.502
- CASOH	-	-	-0.482	-0.482	-0.482	-0.482	-0.482
- DISPLACE HS	-	-	-	-	-0.401	-0.401	-0.401
- DISPLACE RO	-	-	-	-0.359	-	-0.359	-0.359
- DISPLACE SP	-	-	-	-	-	-	-0.260
- MDEA	-	-0.794	-	-	-	-	-
Lean streams	-	0.165	0.045	0.083	0.088	0.126	0.154
- CASOH	-	-	0.045	0.045	0.045	0.045	0.045
- DISPLACE HS	-	-	-	-	0.043	0.043	0.043
- DISPLACE RO	-	-	-	0.038	-	0.038	0.038
- DISPLACE SP	-	-	-	-	-	-	0.028
- MDEA	-	0.165	-	-	-	-	-
NG combustion	-	0.041	-	-	-	-	-
Electricity import	-	0.025	0.138	0.169	0.164	0.195	0.218
- Steel mill	-	0.001	0.100	0.100	0.100	0.100	0.100
- CASOH	-	-	0.038	0.038	0.038	0.038	0.038
- DISPLACE HS	-	-	-	-	0.018	0.018	0.018
- DISPLACE RO	-	-	-	0.022	-	0.022	0.022
- DISPLACE SP	-	-	-	-	-	-	0.023
- ASU for HS	-	-	-	-	0.009	0.009	0.009
- ASU for RO	-	-	-	0.010	-	0.010	0.010
- MDEA	-	0.023	-	-	-	-	-
Electricity export	-0.028	-	-	-	-	-	-
COG export	-	-	-0.080	-0.072	-0.047	-0.022	-
H ₂ -rich mix export	-	-	-0.057	-0.057	-0.057	-0.057	-0.017
Steam export	-	-	-0.018	-	-		
Total	2.107	1.406	1.636	1.334	1.313	1.010	0.834

Table A.2: Breakdown of primary energy consumption for C^4U steel plants. All values are expressed in $[GJ/t_{HRC}]$. The results refer to the scenario in which the carbon intensity of electricity imported from the grid has a carbon footprint equal to $250 \text{ kg}_{CO2}/\text{MWh}_{el}$.

PEC [GJ/t _{HRC}]	Base	Ref.	CASOH	RO	HS	HS-RO	HS-RO-SP
Cocking coal	16.41	16.41	16.41	16.41	16.41	16.41	16.41
PCI coal	5.32	5.32	5.32	5.32	5.32	5.32	5.32
Natural gas	-	0.71	-	-	-	-	-
Electricity	-	0.42	2.36	2.90	2.81	3.35	3.74
- Steel mill	-	0.02	1.72	1.72	1.72	1.72	1.72

Table A.2 (continued).

PEC [GJ/t _{HRC}]	Base	Ref.	CASOH	RO	HS	HS-RO	HS-RO-SP
- CASOH	-	-	0.64	0.64	0.64	0.64	0.64
- DISPLACE HS	-	-	-	-	0.30	0.30	0.30
- DISPLACE RO	-	-	-	0.37	-	0.37	0.37
- DISPLACE SP	-	-	-	-	-	-	0.39
- ASU for HS	-	-	-	-	0.15	0.15	0.15
- ASU for RO	-	-	-	0.16	-	0.16	0.16
- MDEA	-	0.40	-	-	-	-	-
Electricity export	-0.48	-	-	-	-	-	-
COG export	-	-	-1.38	-1.25	-0.81	-0.38	-
H ₂ -rich mix export	-	-	-0.98	-0.98	-0.98	-0.98	-0.30
Steam export	-	-	-0.31	-	-	-	
Total	21.25	22.86	21.42	22.40	22.76	23.72	25.17

Table A.3: Breakdown of levelized cost of hot rolled coil for C^4U steel plants. All values are expressed in $[\notin/t_{HRC}]$. The results refer to the scenario in which electricity and natural gas prices are equal to $125 \notin/MWh_e$ and $50 \notin/MWh_{LHV}$ respectively.

LCOHRC [€/t _{HRC}]	Base	Ref.	CASOH	RO	HS	HS-RO	HS-RO-SP
CAPEX steel mill	118.7	117.4	113.0	114.5	114.7	116.1	116.1
Fix. O&M steel mill	99.1	100.5	97.1	97.1	97.1	97.1	97.1
Var. O&M steel mill	290.7	290.2	288.4	288.4	288.4	288.4	288.4
Misc. OPEX steel mill	14.3	14.3	14.3	14.3	14.3	14.3	14.3
Other O&M costs steel mill	1.8	1.8	1.8	1.8	1.8	1.8	1.8
CO ₂ transport and storage	-	31.8	19.3	33.6	35.3	49.7	60.1
CAPEX CASOH	-	-	28.8	28.8	28.8	28.8	28.8
CAPEX DISPLACE HS	-	-	-	-	8.8	8.8	8.8
CAPEX DISPLACE RO	-	-	-	8.3	-	8.3	8.3
CAPEX DISPLACE SP	-	-	-	-	-	-	8.5
CAPEX MDEA	-	16.1	-	-	-	-	-
Electricity import steel mill	-	0.7	50.1	50.1	50.1	50.1	50.1
Electricity import CASOH	-	-	18.8	18.8	18.8	18.8	18.8
Electricity import DISPLACE HS	-	-	-	-	8.8	8.8	8.8
Electricity import DISPLACE RO	-	-	-	10.8	-	10.8	10.8
Electricity import DISPLACE SP	-	-	-	-	-	-	11.3
Electricity import ASU for HS	-	-	-	-	4.3	4.3	4.3
Electricity import ASU for RO	-	-	-	4.8	-	4.8	4.8
Electricity import MDEA	-	11.6	-	-	-	-	-
Electricity export	-4.6	-	-	-	-	-	-
Natural gas	-	9.8	-	-	-	-	-
Other revenues	-11.6	-11.6	-11.6	-13.2	-13.4	-15.1	-15.1
COG export	-	-	-19.2	-17.3	-11.2	-5.2	-
H ₂ -rich mix export	-	-	-26.0	-26.0	-26.0	-26.0	-7.9
Steam export	-	-	-4.3	-	-		
Total	508.5	582.7	570.5	614.9	620.7	664.7	718.3

Appendix B

In this section the methodology used for the assessment of the CAPEX of CASOH technology is described. One common approach to estimating CAPEX for process equipment is to perform equipment-level costing and then scale those costs according to design capacities or duties. In this work, vendor quotes were collected for the major pieces of equipment (e.g., reactors, compressors, furnaces, heat exchangers, pumps), determining a "base cost" for a certain reference size or capacity. Subsequently, a scaling factor equal to 0.7 was used to capture economies of scale for larger or smaller equipment. This kind of scaling approach is frequently used in early-stage techno-economic assessments. Below an expanded explanation of the methodology used:

- 1. Collecting vendor quotes for reference capacity for each piece of process equipment (e.g., a furnace sized for a specific duty). This establishes the "base cost" for a known reference capacity or size.
- 2. Selecting the scaling exponent to account for how costs change with capacity. In many chemical and process plant applications, an exponent of about 0.7 is common.
- 3. Applying the scaling equation: if C_0 is the cost at the reference capacity S_0 , the cost C for a new capacity S, can be calculated with equation (B.1), where n is the scaling exponent:

$$C = C_0 \times \left(\frac{S}{S_0}\right)^n \tag{B.1}$$

Regarding the reference capacity, duty was selected for furnaces, power for compressors, and volume for reactors. For the reactor's internals, vendors provided a base value of weight (5160 kg). The new value was calculated by multiplying the base weight and the volume ratio between the new and base reactor. For the reactor's valves, we assumed a 70% reduction in the base price provided by vendors because of the consistently lower specifications (temperature and pressure) of the new valves. Table B.1 shows the heat transfer coefficients used to calculate the area of heat exchangers (Sinnot and Towler, 2019). For vessels and auxiliary equipment, it was assumed that the updated cost is 4 times the cost reported by the vendors since four trains in parallel have been designed. In Table 15 the estimation of the total equipment cost of the CASOH technology is detailed. Other equipment include oxygen scavenger, pH control and phosphate packages.

Table B.1: Heat transfer coefficients for different types of heat exchangers.

Heat exchanger type	U (W/m ² K)
Gas to gas	100
Gas to liquid (cooler with saturated liquid changing to steam)	1000
Gas to liquid (cooler with water)	300
Gas to liquid (heater with steam)	1000

Table 15: Details of the total equipment cost of the CASOH technology.

Equipment Class	Code	Stage	Scaling basis	Base value	New value	Unit	Units per plant	Base cost [€]	Cost per equipment (€)	Cost per train [€]	Total cost [€]
Pumps	P-101	CALCINATION	Power	0.01	0.08	MW	4	75,000	487,335	487,335	1,949,340
Pumps	P-102	COOLING WATER	Power	0.01	0.00	MW	4	75,000	39,880	39,880	159,520
Pumps	P-103	COOLING WATER	Power	0.01	0.01	MW	4	75,000	92,082	92,082	368,330
Compressors	C-101	CASOH	Power	1.32	5.84	MW	4	3,960,000	11,213,303	11,213,303	44,853,213
Compressors	C-102	OXIDATION	Power	0.66	0.75	MW	4	1,100,000	1,203,975	1,203,975	4,815,900
Compressors	C-103	CALCINATION	Power	2.52	5.94	MW	4	10,065,000	18,367,016	18,367,016	73,468,065
Compressors	C-104	PURGE	Power	0.28	0.08	MW	4	3,275,000	1,347,859	1,347,859	5,391,436
Furnaces	H-101	CASOH	Duty	2.56	12.22	MW	4	2,067,800	6,178,955	6,178,955	24,715,821
Furnaces	H-102	REDUCTION	Duty	0.12	1.33	MW	4	219,529	1,205,846	1,205,846	4,823,385
Furnaces	H-103	CALCINATION	Duty	0.81	1.78	MW	4	823,860	1,425,426	1,425,426	5,701,704
Reactors	R-101/2/3/4/5	CASOH, REDUCTION, OXIDATION, PURGE, CALCINATION	Volume	41.56	158.80	m3	64	489,078	1,249,896	19,998,340	79,993,362
Internals	R-101/2/ 3/4/5	CASOH, REDUCTION, OXIDATION, PURGE, CALCINATION	Weight	5160	9714	kg	64	19,715	312,474	4,999,586	19,998,343
Special Valves	R-101/2/3/4/5	CASOH, REDUCTION, OXIDATION, PURGE, CALCINATION	-	-	-	-	640	388,235	113,680	18,188,875	72,755,499
Coolers reactor outlet	E-103/4/ 5/6/13	CASOH, REDUCTION, OXIDATION, PURGE, CALCINATION	Area	550	13.55	m^2	64	1,079,600	80,777	1,292,425	5,169,702
Heat Exchangers	E-101	CASOH	Area	116	737.72	m^2	4	58,800	214,675	214,675	858,700
Heat Exchangers	E-102	CASOH	Area	16	208.65	m^2	4	23,000	138,814	138,814	555,255
Coolers	E-107	CALCINATION	Area	564	448.67	m^2	4	341,900	291,308	291,308	1,165,231
Coolers	E-108	CALCINATION	Area	564	291.19	m^2	4	341,900	215,241	215,241	860,963
Coolers	E-109	CASOH	Area	564	676.31	m^2	4	341,900	388,245	388,245	1,552,979
Coolers	E-110	REDUCTION	Area	564	171.29	m^2	4	341,900	148,462	148,462	593,847
Heaters	E-111	CASOH	Area	20	578.00	m^2	4	57,575	606,546	606,546	2,426,186
Heaters	E-112	CALCINATION	Area	132	80.24	m^2	4	93,200	65,778	65,778	263,114
Vessel	V-101	CASOH	-	-	-	-	4	182,000	182,000	182,000	728,000

Equipment Class	Code	Stage	Scaling basis	Base value	New value	Unit	Units per plant	Base cost [€]	Cost per equipment (€)	Cost per train [€]	Total cost [€]
Vessel	V-102	REDUCTION	-	-	-	-	4	182,000	182,000	182,000	728,000
Vessel	V-103	CALCINATION	-	-	-	-	4	1,088,400	1,088,400	1,088,400	4,353,600
Vessel	V-104	CASOH	-	-	-	-	4	182,000	182,000	182,000	728,000
Other equipment			-	-	-	-	4	1,200,000	1,200,000	1,200,000	4,800,000
TOTAL									48,221,973	90,944,372	363,777,495

Bibliography

- Abanades, J.C., Murillo, R., Fernandez, J.R., Grasa, G., Martínez, I., 2010. New CO2 capture process for hydrogen production combining Ca and Cu chemical loops. Environ Sci Technol 44, 6901–6904. https://doi.org/10.1021/es101707t
- Abbas, S.Z., Argyris, P.A., Fernández, J.-R., Abanades, J.C., Spallina, V., 2021. A Ca-Cu Chemical Loop Process for CO2 Capture in Steel Mills: System Performance Analysis, in: Proceedings of the 15th Greenhouse Gas Control Technologies Conference 15-18 March 2021.
- Abdul Quader, M., Ahmed, S., Dawal, S.Z., Nukman, Y., 2016. Present needs, recent progress and future trends of energy-efficient Ultra-Low Carbon Dioxide (CO2) Steelmaking (ULCOS) program. Renewable and Sustainable Energy Reviews 55, 537–549. https://doi.org/https://doi.org/10.1016/j.rser.2015.10.101
- Arasto, A., Tsupari, E., Kärki, J., Lilja, J., Sihvonen, M., 2014. Oxygen blast furnace with CO2 capture and storage at an integrated steel mill—Part I: Technical concept analysis. International Journal of Greenhouse Gas Control 30, 140–147. https://doi.org/https://doi.org/10.1016/j.ijggc.2014.09.004
- Arasto, A., Tsupari, E., Kärki, J., Pisilä, E., Sorsamäki, L., 2013a. Post-combustion capture of CO2 at an integrated steel mill Part I: Technical concept analysis. International Journal of Greenhouse Gas Control 16, 271 277. https://doi.org/10.1016/j.ijggc.2012.08.018
- Arasto, A., Tsupari, E., Kärki, J., Sihvonen, M., Lilja, J., 2013b. Costs and Potential of Carbon Capture and Storage at an Integrated Steel Mill. Energy Procedia 37, 7117–7124. https://doi.org/https://doi.org/10.1016/j.egypro.2013.06.648
- Arias, B., Diego, M.E., Abanades, J.C., Lorenzo, M., Diaz, L., Martínez, D., Alvarez, J., Sánchez-Biezma, A., 2013. Demonstration of steady state CO2 capture in a 1.7MWth calcium looping pilot. International Journal of Greenhouse Gas Control 18, 237–245. https://doi.org/10.1016/j.ijggc.2013.07.014
- Astolfi, M., De Lena, E., Casella, F., Romano, M.C., 2021. Calcium looping for power generation with CO2 capture: The potential of sorbent storage for improved economic performance and flexibility. Appl Therm Eng 194, 117048. https://doi.org/10.1016/j.applthermaleng.2021.117048
- Baker, R.W., Freeman, B., Kniep, J., Huang, Y.I., Merkel, T.C., 2018. CO2 Capture from Cement Plants and Steel Mills Using Membranes. Ind Eng Chem Res 57, 15963–15970. https://doi.org/10.1021/acs.iecr.8b02574
- Biermann, M., Ali, H., Sundqvist, M., Larsson, M., Normann, F., Johnsson, F., 2019. Excess heat-driven carbon capture at an integrated steel mill Considerations for capture cost optimization. International Journal of Greenhouse Gas Control 91, 102833. https://doi.org/10.1016/j.jiggc.2019.102833
- Birat, J.-P., 2010. 16 Carbon dioxide (CO2) capture and storage technology in the iron and steel industry, in: Maroto-Valer, M.M. (Ed.), Developments and Innovation in Carbon Dioxide (CO2) Capture and Storage Technology. Woodhead Publishing, pp. 492–521. https://doi.org/https://doi.org/10.1533/9781845699574.5.492
- Budhi, Y.W., Suganda, W., Irawan, H.K., Restiawaty, E., Miyamoto, M., Uemiya, S., Nishiyama, N., van Sint Annaland, M., 2020. Hydrogen separation from mixed gas (H2, N2) using Pd/Al2O3 membrane under forced unsteady state operations. Int J Hydrogen Energy 45, 9821–9835. https://doi.org/https://doi.org/10.1016/j.ijhydene.2020.01.235
- C4U website [WWW Document], n.d. URL https://c4u-project.eu/ (accessed 11.12.24).
- Chamchan, N., Chang, J.-Y., Hsu, H.-C., Kang, J.-L., Wong, D.S.H., Jang, S.-S., Shen, J.-F., 2017. Comparison of rotating packed bed and packed bed absorber in pilot plant and model simulation for CO2 capture. J Taiwan Inst Chem Eng 73, 20–26. https://doi.org/https://doi.org/10.1016/j.jtice.2016.08.046
- Cheng, H.-H., Shen, J.-F., Tan, C.-S., 2010. CO2 capture from hot stove gas in steel making process. International Journal of Greenhouse Gas Control 4, 525–531. https://doi.org/https://doi.org/10.1016/j.ijggc.2009.12.006
- Chisalita, D.-A., Petrescu, L., Cobden, P., van Dijk, H.A.J. (Eric), Cormos, A.-M., Cormos, C.-C., 2019. Assessing the environmental impact of an integrated steel mill with post-combustion CO2 capture and storage using the LCA methodology. J Clean Prod 211, 1015–1025. https://doi.org/https://doi.org/10.1016/j.jclepro.2018.11.256

- Chung, W., Roh, K., Lee, J.H., 2018a. Design and evaluation of CO2 capture plants for the steelmaking industry by means of amine scrubbing and membrane separation. International Journal of Greenhouse Gas Control 74, 259–270. https://doi.org/https://doi.org/10.1016/j.ijggc.2018.05.009
- Chung, W., Roh, K., Lee, J.H., 2018b. Design and evaluation of CO2 capture plants for the steelmaking industry by means of amine scrubbing and membrane separation. International Journal of Greenhouse Gas Control 74, 259–270. https://doi.org/https://doi.org/10.1016/j.ijggc.2018.05.009
- Cormos, A.-M., Dragan, S., Petrescu, L., Sandu, V., Cormos, C.-C., 2020a. Techno-Economic and Environmental Evaluations of Decarbonized Fossil-Intensive Industrial Processes by Reactive Absorption & Adsorption CO2 Capture Systems. Energies (Basel) 13. https://doi.org/10.3390/en13051268
- Cormos, A.-M., Dumbrava, I., Cormos, C.-C., 2020b. Evaluation of techno-economic performance for decarbonized hydrogen and power generation based on glycerol thermo-chemical looping cycles. Appl Therm Eng 179, 115728. https://doi.org/https://doi.org/10.1016/j.applthermaleng.2020.115728
- Cormos, C.-C., 2016. Evaluation of reactive absorption and adsorption systems for post-combustion CO2 capture applied to iron and steel industry. Appl Therm Eng 105, 56–64. https://doi.org/https://doi.org/10.1016/j.applthermaleng.2016.05.149
- Danloy G., Berthelemot A., Grant M., Borlée J., Sert D., van der Stel J., Jak H., Dimastromatteo V., Hallin M., Eklund N., Edberg N., Sundqvist L., Sköld B.-E., Lin R., Feiterna A., Korthas B., Müller F., Feilmayr C., Habermann A., 2009. ULCOS Pilot testing of the Low-CO2 Blast Furnace process at the experimental BF in Luleå. Rev. Met. Paris 106, 1–8. https://doi.org/10.1051/metal/2009008
- De Falco, M., Marrelli, L., Iaquaniello, G., 2011. Membrane reactors for hydrogen production process. Springer-Verlag, London.
- Fernández, J.R., Martínez, I., Abanades, J.C., Romano, M.C., 2017. Conceptual design of a Ca–Cu chemical looping process for hydrogen production in integrated steelworks. Int J Hydrogen Energy 42, 11023–11037. https://doi.org/https://doi.org/10.1016/j.ijhydene.2017.02.141
- Fernández, J.R., Spallina, V., Abanades, J.C., 2020. Advanced packed-bed Ca-Cu looping process for the CO2 capture from steel mill off-gases. Front Energy Res 8. https://doi.org/10.3389/fenrg.2020.00146
- Gazzani, M., Romano, M.C., Manzolini, G., 2015. CO2 capture in integrated steelworks by commercial-ready technologies and SEWGS process. International Journal of Greenhouse Gas Control 41, 249–267. https://doi.org/https://doi.org/10.1016/j.ijggc.2015.07.012
- Gentile, G., Bonalumi, D., Pieterse, J.A.Z., Sebastiani, F., Lucking, L., Manzolini, G., 2022. Techno-economic assessment of the FReSMe technology for CO2 emissions mitigation and methanol production from steel plants. Journal of CO2 Utilization 56. https://doi.org/10.1016/j.jcou.2021.101852
- Goto, K., Okabe, H., Chowdhury, F.A., Shimizu, S., Fujioka, Y., Onoda, M., 2011. Development of novel absorbents for CO2 capture from blast furnace gas. International Journal of Greenhouse Gas Control 5, 1214–1219. https://doi.org/https://doi.org/10.1016/j.ijggc.2011.06.006
- Grasa, G., Díaz, M., Fernández, J.R., Amieiro, A., Brandt, J., Abanades, J.C., 2023. Blast furnace gas decarbonisation through Calcium Assisted Steel-mill Off-gas Hydrogen production. Experimental and modelling approach. Chemical Engineering Research and Design 191, 507–522. https://doi.org/https://doi.org/10.1016/j.cherd.2023.01.047
- Guo, Z., Wang, Q., Fang, M., Luo, Z., Cen, K., 2014. Thermodynamic and economic analysis of polygeneration system integrating atmospheric pressure coal pyrolysis technology with circulating fluidized bed power plant. Appl Energy 113, 1301–1314. https://doi.org/https://doi.org/10.1016/j.apenergy.2013.08.086
- Halmann, M., Steinfeld, A., 2015. Reforming of Blast Furnace Gas with Methane, Steam, and Lime for Syngas Production and CO2 Capture: A Thermodynamic Study. Mineral Processing and Extractive Metallurgy Review 36, 7–12. https://doi.org/10.1080/08827508.2013.793682
- Hamelinck, C., Bunse, M., 2022. Carbon footprint of methanol.
- Hasan, M.M.F., Baliban, R.C., Elia, J.A., Floudas, C.A., 2012. Modeling, Simulation, and Optimization of Postcombustion CO2 Capture for Variable Feed Concentration and Flow Rate. 1. Chemical Absorption and Membrane Processes. Ind Eng Chem Res 51, 15642–15664. https://doi.org/10.1021/ie301571d
- Ho, M.T., Allinson, G.W., Wiley, D.E., 2011. Comparison of MEA capture cost for low CO2 emissions sources in Australia. International Journal of Greenhouse Gas Control 5, 49–60. https://doi.org/https://doi.org/10.1016/j.ijggc.2010.06.004

- Ho, M.T., Bustamante, A., Wiley, D.E., 2013. Comparison of CO2 capture economics for iron and steel mills. International Journal of Greenhouse Gas Control 19, 145–159. https://doi.org/10.1016/j.ijggc.2013.08.003
- Huijgen, W.J.J., Comans, R.N.J., Witkamp, G.-J., 2007. Cost evaluation of CO2 sequestration by aqueous mineral carbonation. Energy Convers Manag 48, 1923–1935. https://doi.org/https://doi.org/10.1016/j.enconman.2007.01.035
- IEAGHG Technical Report, 2017. Techno-Economic Evaluation of HYCO Plant Integrated to Ammonia/Urea or Methanol Production with CCS.
- IEAGHG Technical Report, 2013. Iron and Steel CCS Study (Techno-economics integrated steel mill).
- International Energy Agency, 2020. Iron and Steel Technology Roadmap Towards more sustainable steelmaking Part of the Energy Technology Perspectives series.
- International industrial energy prices GOV.UK [WWW Document], n.d. URL https://www.gov.uk/government/statistical-data-sets/international-industrial-energy-prices (accessed 4.10.24).
- Jeon, J.-Y., Park, B.-R., Kim, J.-H., 2022. Numerical Simulation and Optimization of 4-Component LDG Separation in the Steelmaking Industry Using Polysulfone Hollow Fiber Membranes. Membranes (Basel) 12. https://doi.org/10.3390/membranes12010097
- Jin, P., Jiang, Z., Bao, C., Hao, S., Zhang, X., 2017. The energy consumption and carbon emission of the integrated steel mill with oxygen blast furnace. Resour Conserv Recycl 117, 58–65. https://doi.org/https://doi.org/10.1016/j.resconrec.2015.07.008
- Jin, P., Jiang, Z., Bao, C., Lu, Y., Zhang, J., Zhang, X., 2016. Mathematical Modeling of the Energy Consumption and Carbon Emission for the Oxygen Blast Furnace with Top Gas Recycling. Steel Res Int 87, 320–329. https://doi.org/10.1002/srin.201500054
- Katayama, K., Bahzad, H., Boot-Handford, M., Patzschke, C.F., Fennell, P.S., 2020. Process Integration of Chemical Looping Water Splitting with a Sintering Plant for Iron Making. Ind Eng Chem Res 59, 7021–7032. https://doi.org/10.1021/acs.iecr.9b05945
- Khallaghi, N., Abbas, S.Z., Manzolini, G., De Coninck, E., Spallina, V., 2022. Techno-economic assessment of blast furnace gas pre-combustion decarbonisation integrated with the power generation. Energy Convers Manag 255. https://doi.org/10.1016/j.enconman.2022.115252
- Kim, H., Lee, J., Lee, S., Lee, I.-B., Park, J., Han, J., 2015. Economic process design for separation of CO2 from the off-gas in ironmaking and steelmaking plants. Energy 88, 756–764. https://doi.org/https://doi.org/10.1016/j.energy.2015.05.093
- Lewis, E., McNaul, S., Jamieson, M., Henriksen, M.S., Matthews, H.S., Walsh, L., Grove, J., Shultz, T., Skone, T.J., Stevens, R., 2022. Comparison of Commercial, State-of-the-Art, Fossil-Based Hydrogen Production Technologies. United States. https://doi.org/10.2172/1862910
- Li, R., Lian, S., Zhang, Z., Song, C., Han, R., Liu, Q., 2022. Techno-economic evaluation of a novel membrane-cryogenic hybrid process for carbon capture. Appl Therm Eng 200, 117688. https://doi.org/https://doi.org/10.1016/j.applthermaleng.2021.117688
- Li, Z., Yi, Q., Zhang, Y., Zhou, H., Zhao, Y., Huang, Y., Gao, D., Hao, Y., 2020. Numerical study and design strategy for a low emission coke oven system using oxy-fuel combustion of coke oven gas. J Clean Prod 252, 119656. https://doi.org/https://doi.org/10.1016/j.jclepro.2019.119656
- Lu, H.T., Li, W., Miandoab, E.S., Kanehashi, S., Hu, G., 2021. The opportunity of membrane technology for hydrogen purification in the power to hydrogen (P2H) roadmap: a review. Front Chem Sci Eng 15, 464–482. https://doi.org/10.1007/s11705-020-1983-0
- Luca, A.-V., Petrescu, L., 2021. Membrane technology applied to steel production: Investigation based on process modelling and environmental tools. J Clean Prod 294, 126256. https://doi.org/https://doi.org/10.1016/j.jclepro.2021.126256
- Luo, M., Wang, C., Yi, Y., Liu, K., Cai, J., Wang, Q., 2018. Power Generation from Coke Oven Gas Using Chemical Looping Combustion: Thermodynamic Simulation. Chem Eng Technol 41, 524–531. https://doi.org/https://doi.org/10.1002/ceat.201700322
- Manzolini, G., Giuffrida, A., Cobden, P.D., van Dijk, H.A.J., Ruggeri, F., Consonni, F., 2020. Techno-economic assessment of SEWGS technology when applied to integrated steel-plant for CO2 emission mitigation. International Journal of Greenhouse Gas Control 94. https://doi.org/10.1016/j.ijggc.2019.102935

- Manzolini, G., Giuffrida, A., Zecca, N., Lücking, L., Pieterse, J.A.Z., Sebastiani, F., Van Dijk, E., 2022. DISPLACE technology to efficiently decarbonize steel industry, in: Proceedings of the 16th Greenhouse Gas Control Technologies Conference (GHGT-16).
- Martinez Castilla, G., Biermann, M., Montañés, R.M., Normann, F., Johnsson, F., 2019. Integrating carbon capture into an industrial combined-heat-and-power plant: performance with hourly and seasonal load changes. International Journal of Greenhouse Gas Control 82, 192–203. https://doi.org/https://doi.org/10.1016/j.ijggc.2019.01.015
- Martínez, I., Fernández, J.R., Abanades, J.C., Romano, M.C., 2018a. Integration of a fluidised bed Ca–Cu chemical looping process in a steel mill. Energy 163, 570–584. https://doi.org/https://doi.org/10.1016/j.energy.2018.08.123
- Martínez, I., Fernández, J.R., Abanades, J.C., Romano, M.C., 2018b. Integration of a fluidised bed Ca–Cu chemical looping process in a steel mill. Energy 163, 570–584. https://doi.org/https://doi.org/10.1016/j.energy.2018.08.123
- Martínez, I., Fernández, J.R., Martini, M., Gallucci, F., van Sint Annaland, M., Romano, M.C., Abanades, J.C., 2019. Recent progress of the Ca-Cu technology for decarbonisation of power plants and carbon intensive industries. International Journal of Greenhouse Gas Control 85, 71–85. https://doi.org/https://doi.org/10.1016/j.ijggc.2019.03.026
- Masoudi Soltani, S., Lahiri, A., Bahzad, H., Clough, P., Gorbounov, M., Yan, Y., 2021. Sorption-enhanced Steam Methane Reforming for Combined CO2 Capture and Hydrogen Production: A State-of-the-Art Review. Carbon Capture Science & Technology 1, 100003. https://doi.org/10.1016/j.ccst.2021.100003
- Niel, J., Weiss, B., Wukovits, W., 2022. Model of an iron ore sinter plant with selective waste gas recirculation. Carbon Resources Conversion 5, 71–83. https://doi.org/https://doi.org/10.1016/j.crcon.2022.01.001
- Oko, E., Zacchello, B., Wang, M., Fethi, A., 2018. Process analysis and economic evaluation of mixed aqueous ionic liquid and monoethanolamine (MEA) solvent for CO2 capture from a coke oven plant. Greenhouse Gases: Science and Technology 8, 686–700. https://doi.org/https://doi.org/10.1002/ghg.1772
- Onarheim, K., Arasto, A., 2016. Staged implementation of alternative processes in an existing integrated steel mill for improved performance and reduced CO2 emissions Part I: Technical concept analysis. International Journal of Greenhouse Gas Control 45, 163–171. https://doi.org/https://doi.org/10.1016/j.ijggc.2015.12.008
- Perpiñán, J., Peña, B., Bailera, M., Eveloy, V., Kannan, P., Raj, A., Lisbona, P., Romeo, L.M., 2023. Integration of carbon capture technologies in blast furnace based steel making: A comprehensive and systematic review. Fuel 336, 127074. https://doi.org/https://doi.org/10.1016/j.fuel.2022.127074
- Petrescu, L., Chisalita, D.-A., Cormos, C.-C., Manzolini, G., Cobden, P., van Dijk, H.A.J., 2019. Life Cycle Assessment of SEWGS Technology Applied to Integrated Steel Plants. Sustainability 11. https://doi.org/10.3390/su11071825
- Qie, Y., Lyu, Q., Lan, C., Zhang, S., 2020. Energy Conservation and CO2 Abatement Potential of a Gas-injection Blast Furnace. High Temperature Materials and Processes 39, 96–106. https://doi.org/doi:10.1515/htmp-2020-0031
- Quader, M.A., Ahmed, Shamsuddin, Raja Ghazilla, R.A., Ahmed, Shameem, Dahari, M., 2016. Evaluation of criteria for CO2 capture and storage in the iron and steel industry using the 2-tuple DEMATEL technique. J Clean Prod 120, 207–220. https://doi.org/https://doi.org/10.1016/j.jclepro.2015.10.056
- Ramírez-Santos, Á.A., Bozorg, M., Addis, B., Piccialli, V., Castel, C., Favre, E., 2018. Optimization of multistage membrane gas separation processes. Example of application to CO2 capture from blast furnace gas. J Memb Sci 566, 346–366. https://doi.org/https://doi.org/10.1016/j.memsci.2018.08.024
- Remus, R., Aguado-Monsonet, M.A., Roudier, S., Delgado Sancho, L., 2013. Best Available Techniques (BAT) Reference Document for Iron and Steel Production Industrial Emissions Directive 2010/75/EU (Integrated Pollution Prevention and Control).
- Sahu, R.K., Roy, S.K., Sen, P.K., 2015. Applicability of Top Gas Recycle Blast Furnace with Downstream Integration and Sequestration in an Integrated Steel Plant. Steel Res Int 86, 502–516. https://doi.org/https://doi.org/10.1002/srin.201400196
- Sandhya Rani, S.L., Kumar, R.V., 2021. Insights on applications of low-cost ceramic membranes in wastewater treatment: A mini-review. Case Studies in Chemical and Environmental Engineering 4, 100149. https://doi.org/https://doi.org/10.1016/j.cscee.2021.100149

- She, X., An, X., Wang, J., Xue, Q., Kong, L., 2017. Numerical analysis of carbon saving potential in a top gas recycling oxygen blast furnace. Journal of Iron and Steel Research International 24, 608–616. https://doi.org/10.1016/S1006-706X(17)30092-4
- Sinnot, R., Towler, G., 2019. Chemical Engineering Design, 6th ed. Butterworth-Heinemann.
- Smith, E., Morris, J., Kheshgi, H., Teletzke, G., Herzog, H., Paltsev, S., 2021. The cost of CO2 transport and storage in global integrated assessment modeling. International Journal of Greenhouse Gas Control 109, 103367. https://doi.org/https://doi.org/10.1016/j.ijggc.2021.103367
- Ströhle, J., Junk, M., Kremer, J., Galloy, A., Epple, B., 2014. Carbonate looping experiments in a 1 MWth pilot plant and model validation. Fuel 127, 13–22. https://doi.org/10.1016/j.fuel.2013.12.043
- Sun, Zhao, Liu, J., Sun, Zhiqiang, 2020. Synergistic decarbonization and desulfurization of blast furnace gas via a novel magnesium-molybdenum looping process. Fuel 279, 118418. https://doi.org/https://doi.org/10.1016/j.fuel.2020.118418
- Sundqvist, M., Biermann, M., Normann, F., Larsson, M., Nilsson, L., 2018. Evaluation of low and high level integration options for carbon capture at an integrated iron and steel mill. International Journal of Greenhouse Gas Control 77, 27–36. https://doi.org/https://doi.org/10.1016/j.ijggc.2018.07.008
- Tian, S., Jiang, J., Zhang, Z., Manovic, V., 2018. Inherent potential of steelmaking to contribute to decarbonisation targets via industrial carbon capture and storage. Nat Commun 9, 4422. https://doi.org/10.1038/s41467-018-06886-8
- Tsupari, E., Kärki, J., Arasto, A., Lilja, J., Kinnunen, K., Sihvonen, M., 2015. Oxygen blast furnace with CO2 capture and storage at an integrated steel mill Part II: Economic feasibility in comparison with conventional blast furnace highlighting sensitivities. International Journal of Greenhouse Gas Control 32, 189–196. https://doi.org/https://doi.org/10.1016/j.ijggc.2014.11.007
- Tsupari, E., Kärki, J., Arasto, A., Pisilä, E., 2013. Post-combustion capture of CO2 at an integrated steel mill Part II: Economic feasibility. International Journal of Greenhouse Gas Control 16, 278 286. https://doi.org/10.1016/j.ijggc.2012.08.017
- van Dijk, H.A.J., Cobden, P.D., Lukashuk, L., de Water, L. van, Lundqvist, M., Manzolini, G., Cormos, C.-C., van Dijk, C., Mancuso, L., Johns, J., Bellqvist, D., 2018. STEPWISE Project: Sorption-Enhanced Water-Gas Shift Technology to Reduce Carbon Footprint in the Iron and Steel Industry. Johnson Matthey Technology Review 62, 395–402. https://doi.org/https://doi.org/10.1595/205651318X15268923666410
- Wiley, D.E., Ho, M.T., Bustamante, A., 2011. Assessment of opportunities for CO2 capture at iron and steel mills:

 An Australian perspective. Energy Procedia 4, 2654–2661.

 https://doi.org/https://doi.org/10.1016/j.egypro.2011.02.165
- Wright, A.D., White, V., Hufton, J.R., Quinn, R., Cobden, P.D., van Selow, E.R., 2011. CAESAR: Development of a SEWGS model for IGCC. Energy Procedia 4, 1147–1154. https://doi.org/https://doi.org/10.1016/j.egypro.2011.01.167
- Xiang, D., Zhao, S., 2018. Parameter optimization and thermodynamic analysis of COG direct chemical looping hydrogen processes. Energy Convers Manag 172, 1–8. https://doi.org/https://doi.org/10.1016/j.enconman.2018.07.007
- Xie, H., Yu, Q., Zhang, Y., Zhang, J., Liu, J., Qin, Q., 2017. New process for hydrogen production from raw coke oven gas via sorption-enhanced steam reforming: Thermodynamic analysis. Int J Hydrogen Energy 42, 2914–2923. https://doi.org/https://doi.org/10.1016/j.ijhydene.2016.12.046
- Yan, Y., Manovic, V., Anthony, E.J., Clough, P.T., 2020. Techno-economic analysis of low-carbon hydrogen production by sorption enhanced steam methane reforming (SE-SMR) processes. Energy Convers Manag 226. https://doi.org/10.1016/j.enconman.2020.113530
- Yun, S., Jang, M.-G., Kim, J.-K., 2021. Techno-economic assessment and comparison of absorption and membrane CO2 capture processes for iron and steel industry. Energy 229, 120778. https://doi.org/https://doi.org/10.1016/j.energy.2021.120778
- Zecca, N., Cobden, P.D., Lücking, L., Manzolini, G., 2023. SEWGS integration in a direct reduction steelmaking process for CO2 mitigation. International Journal of Greenhouse Gas Control 130. https://doi.org/https://doi.org/10.1016/j.ijggc.2023.103991

- Zecca, N., Lücking, L., Chisăliță, D.-A., Boon, J., van Dijk, H.A.J., Pieterse, J.A.Z., Giuffrida, A., Manzolini, G., 2025. DISPLACE Post-Combustion Carbon Capture Technology Integration in a Steel Plant for CO2 Reduction. J Clean Prod 144739. https://doi.org/https://doi.org/10.1016/j.jclepro.2025.144739
- Zuo Guangqing, Hirsch A., 2009. The Trial of the Top Gas Recycling Blast Furnace at LKAB's EBF and Scale-up. Rev. Met. Paris 106, 387–392. https://doi.org/10.1051/metal/2009067